

Efficient Federated Meta-Learning over Multi-Access Wireless Networks

Sheng Yue, *Student Member, IEEE*, Ju Ren, *Member, IEEE*, Jiang Xin, *Student Member, IEEE*, Deyu Zhang, *Member, IEEE*, Yaoxue Zhang, *Senior Member, IEEE*, and Weihua Zhuang, *Fellow, IEEE*

arXiv:2108.06453v1 [cs.LG] 14 Aug 2021

Abstract—Federated meta-learning (FML) has emerged as a promising paradigm to cope with the data limitation and heterogeneity challenges in today’s edge learning arena. However, its performance is often limited by slow convergence and corresponding low communication efficiency. Besides, since the wireless bandwidth and IoT devices’ energy capacity are usually insufficient, it is crucial to control the resource allocation and energy consumption when deploying FML in realistic wireless networks. To overcome these challenges, in this paper, we first rigorously analyze each device’s contribution to the global loss reduction in each round and develop an FML algorithm (called NUFM) with a non-uniform device selection scheme to accelerate the convergence. After that, we formulate a resource allocation problem integrating NUFM in multi-access wireless systems to jointly improve the convergence rate and minimize the wall-clock time along with energy cost. By deconstructing the original problem step by step, we devise a joint device selection and resource allocation strategy (called URAL) to solve the problem, and provide theoretical guarantees. Further, we show that the computational complexity of NUFM can be reduced from $O(d^2)$ to $O(d)$ (with d being the model dimension) via combining two first-order approximation techniques. Extensive simulation results demonstrate the effectiveness and superiority of the proposed methods by comparing to the existing baselines.

Index Terms—Federated meta-learning, multi-access systems, device selection, resource allocation, efficiency

I. INTRODUCTION

THE integration of Artificial Intelligence (AI) and Internet-of-Things (IoT) led to a proliferation of studies on edge intelligence, aiming at pushing AI frontiers to the wireless network edge proximal to IoT devices and data sources [1], [2]. It is expected that edge intelligence will reduce time-to-action latency down to milliseconds for AIoT applications while minimizing network bandwidth and offering great security guarantees [3]. However, a general consensus is that a single IoT device can hardly realize edge intelligence due to its limited computational and storage capabilities. Accordingly, it is natural to rely on collaboration in edge learning, whereby IoT devices work together to accomplish computation-intensive tasks [4].

Building on a synergy of federated learning [5] and meta-learning [6], [7], federated meta-learning (FML) has been

Sheng Yue, Jiang Xin, Deyu Zhang are with the School of Computer Science and Engineering, Central South University, Changsha, 410083 China. Emails: {yue.sheng, xinjiang, zdy876}@csu.edu.cn.

Ju Ren and Yaoxue Zhang are with the Department of Computer Science and Technology, Tsinghua University, Beijing, 100084 China. Emails: {renju.yxhang}@tsinghua.edu.cn.

Weihua Zhuang is with the Department of Electrical and Computer Engineering, University of Waterloo, Waterloo, ON, Canada. Email: wzhuang@uwaterloo.ca.

proposed under a common theme of fostering edge-edge collaboration [8]–[10]. In FML, IoT devices join forces to learn an *initial shared model* under the orchestration of a central server such that current or new devices can quickly adapt the learned model to their local datasets via one or a few gradient descent steps. Notably, FML can keep all the benefits of the federated learning paradigm (such as simplicity, data security, and flexibility) while giving a more personalized model for each device to capture the difference among tasks [11]. Therefore, FML has emerged as a promising approach to tackle the heterogeneity challenges in federated learning and facilitate efficient edge learning [12].

Despite its promising benefits, FML comes with some new challenges. On the one hand, the number of participated devices can be enormous. The randomly uniform device selection, often done in the existing methods, naturally leads to a low convergence speed [11], [13]. Although recent studies [14]–[16] have characterized the convergence of federated learning and proposed non-uniform device selection mechanisms, they cannot be directly applied to FML problems due to the bias and high-order information in the stochastic gradients. On the other hand, the performance of FML in a wireless environment is highly related to its wall-clock time, including the computation time (with respect to local data sizes and devices’ CPU types) and communication time (depending on channel gains, interference, and transmission power) [17]. If not being properly controlled, large wall-clock time would cause unexpected training delay and communication inefficiency. In addition, due to the limited power capacity of IoT devices, energy consumption should also be well managed to ensure system sustainability and stability [16]. Thus, for the purpose of efficiently deploying FML in today’s wireless systems, the strategy of device selection and resource allocation must be carefully crafted not only to accelerate the learning process, but also control the wall-clock time of training and energy cost in edge devices. Unfortunately, despite the importance, scant attention has been paid to these aspects in the current literature.

To fill this gap, in this paper, we tackle the above-mentioned challenges in two steps: 1) We develop an algorithm (called NUFM) with a non-uniform device selection scheme to improve the convergence rate of vanilla FML algorithm; 2) based on NUFM, a resource allocation strategy (called URAL) is proposed, jointly optimizing the convergence speed, wall-clock time, and energy consumption in the context of multi-access wireless systems. More specifically, we first rigorously quantify each device’s contribution to the convergence of FML

via deriving a tight lower bound on the one-round global loss decrease. Based on the quantitative insights, we give the non-uniform device selection scheme that maximizes the loss reduction per round, followed by the NUFM algorithm. Then, we formulate a resource allocation problem for NUFM over wireless networks, capturing the trade-offs among convergence, wall-clock time, and energy cost. To solve this problem, we exploit its special structure and decompose it into two sub-problems. The first one is to minimize the computation time via controlling devices' CPU-cycle frequencies, which is solved optimally based on the analysis of device heterogeneity's effect on the objective. The second sub-problem aims at optimizing the resource block allocation and transmission power management. It is a non-convex mixed-integer non-linear programming (MINLP) problem that is non-trivial to derive a closed-form solution. Thus, after deconstructing the problem step by step, we devise an iterative method to solve it and provide a convergence guarantee.

In summary, our main contributions are three-fold.

- We provide a theoretical characterization of each device's contribution to the convergence of FML in each round, via establishing a tight lower bound on the one-round reduction of expected global loss. Using this quantitative result, we develop NUFM, a fast-convergent FML algorithm with the non-uniform device selection scheme.
- To embed NUFM in the context of multi-access wireless systems, we cast a resource allocation problem, capturing the trade-offs among the convergence, wall-clock time, and energy consumption. By decomposing the original problem into two sub-problems and deconstructing sub-problems step by step, we propose a joint device selection and resource allocation algorithm (namely URAL) to solve the problem effectively with theoretical guarantees.
- To reduce the computational complexity, we further integrate our proposed algorithms with two first-order approximation techniques in the literature [11], by which the complexity of a one-step update in NUFM can be reduced from $O(d^2)$ down to $O(d)$. We also show that our theoretical results still hold in these cases.
- We provide extensive simulation results on challenging real-world benchmarks (*i.e.*, FMNIST, CIFAR100, and ImageNet) to demonstrate the efficacy of our methods.

The remainder of this paper is organized in the following way. Section II first briefly reviews the related work. Section III introduces the FML problem and standard algorithm. We present the non-uniform device selection scheme in Section IV and adapt the scheme in wireless networks in Section V. Finally, Section VI shows the extension to first-order approximation techniques, followed by the simulation results in VII and a conclusion drawn in Section VIII.

II. RELATED WORK

Federated learning (FL) [5] has been proposed as a promising technique to facilitate edge-edge collaborative learning. However, due to the heterogeneity in devices, models, and data distributions, a shared global model often fails to capture the personal information of each device, leading to performance degradation in inference or classification [12], [18], [19].

Very recently, based on the advances in meta-learning [6], [7], federated meta-learning (FML) has garnered much attention, which aims to learn a personalized model for each device to cope with the heterogeneity challenges [8]–[11], [13], [20], [21]. Chen *et al.* [8] first introduce an FML method called FedMeta, integrating the model-agnostic meta-learning (MAML) algorithm [6] into the federated learning framework. They show that FML can significantly improve the performance of FedAvg [5]. Jiang *et al.* [9] analyze the connection between FedAvg and MAML, and empirically demonstrate that FML enables better and more stable personalized performance. From a theoretical perspective, Lin *et al.* [10] analyze the convergence properties and computational complexity of FML with strongly convex loss functions and exact gradients. Fallah *et al.* [11] further provide the convergence guarantees in non-convex cases with stochastic gradients. Different from the above gradient descent-based approaches, another recent work [13] develops an ADMM-based FML method and gives its convergence guarantee under non-convex cases. However, due to selecting devices uniformly at random, the existing FML algorithms often suffer from slow convergence and low communication efficiency [11]. Besides, deploying FML in practical wireless systems also calls for effective resource allocation strategies [17], but it lies beyond the scope of existing FML literature.

There has been a significant body of works placing interests in convergence improvement and resource allocation for FL [15]–[17], [22]–[31]. Regarding the convergence improvement, Nguyen *et al.* [15] propose a fast-convergent FL algorithm, called FOLB, which achieves a near-optimal lower bound for the overall loss decrease in each round. We note that while the idea of NUFM is similar to [15], the lower bound for FML is derived from a completely different technical path due to the inherent complexity in the local update. To minimize the convergence time, a probabilistic device selection scheme for FL is designed in [26], which assigns high probabilities to the devices with large effects on the global model. Ren *et al.* [27] investigate the batchsize selection strategy for accelerating the FL training process. Karimireddy *et al.* [31] employ the variance reduction technique to develop a new FL algorithm, called SCAFFOLD. Based on momentum methods, Yu *et al.* [28] give an FL algorithm with linear speedup property. Regarding the resource allocation in FL, Dinh *et al.* [17] embed FL in wireless networks, considering the trade-offs between training time and energy consumption. However, they assume all devices would participate in the whole training process. From a long-term perspective, Xu *et al.* [29] empirically investigate the device selection scheme jointly with bandwidth allocation for FL, using the Lyapunov optimization technology. Chen *et al.* [16] investigate a device selection problem with “hard” resource constraints to enable the implementation of FL over wireless networks. Wang *et al.* [30] propose a control algorithm to determine the best trade-off between the local update and global aggregation under a resource budget.

Although extensive research has been carried out on FL, researchers have not treated FML in much detail. In particular, the existing FL acceleration techniques cannot be directly

applied to FML due to the high-order information and biased stochastic gradients in the local update phases¹ (see Lemma 2 in Section IV). At the same time, device selection and resource allocation require crafting jointly [8], rather than simply plugging the existing strategies in.

III. PRELIMINARIES AND ASSUMPTIONS

In this section, we introduce federated meta-learning, including the learning problem, standard algorithm, and assumptions for theoretical analysis.

A. Federated Meta-Learning Problem

We consider a set \mathcal{N} of users that are all connected to a server. Each user $i \in \mathcal{N}$ has a labeled dataset $\mathcal{D}_i = \{\mathbf{x}_i^j, \mathbf{y}_i^j\}_{j=1}^{D_i}$ that can be accessed only by itself. Here, the tuple $(\mathbf{x}_i^j, \mathbf{y}_i^j) \in \mathcal{X} \times \mathcal{Y}$ is a data sample with input \mathbf{x}_i^j and label \mathbf{y}_i^j , and follows an unknown underlying distribution P_i . For user i , the loss function of a model parameter $\theta \in \mathbb{R}^d$ is defined as $\ell_i(\theta; \mathbf{x}, \mathbf{y})$, which measures the error of the model θ in predicting the true label \mathbf{y} given the input \mathbf{x} .

Federated meta-learning (FML) looks for a good model initialization (also called meta-model) such that the well-performed models of different users can be quickly obtained via one or a few gradient descent steps. More specially, FML aims to solve the following problem

$$\min_{\theta \in \mathbb{R}^d} F(\theta) := \frac{1}{n} \sum_{i \in \mathcal{N}} f_i(\theta - \alpha \nabla \ell_i(\theta)), \quad (1)$$

where f_i represents the expected loss function over the data distribution of user i , *i.e.*, $f_i(\theta) := \mathbb{E}_{(\mathbf{x}, \mathbf{y}) \sim P_i} [\ell_i(\theta; \mathbf{x}, \mathbf{y})]$, and $n = |\mathcal{N}|$ is the number of users. The advantages of this formulation are two-fold: 1) It gives a personalized solution that can capture the heterogeneity between existing users; 2) the meta-model can quickly adapt to new users via slightly updating it with respect to their own data. Clearly, FML well fits edge learning cases, where edge devices have insufficient computing power and limited data samples.

Next, we give the standard FML algorithm in the literature.

B. Standard Algorithm

Similar to federated learning, vanilla FML algorithm solves (1) in two repeating steps: *local update* and *global aggregation* [11], which are depicted below.

- *Local update*: At the beginning of each round k , the server first sends the current global model θ^k to a fraction of users \mathcal{N}_k chosen uniformly at random with size n . Then, each user $i \in \mathcal{N}_k$ updates the received model based on its meta-function $F_i(\theta) := f_i(\theta - \alpha \nabla \ell_i(\theta))$ by running $\tau \geq 1$ steps of stochastic gradient descent locally (also called mini-batch gradient descent), *i.e.*,

$$\theta_i^{k,t+1} = \theta_i^{k,t} - \beta \tilde{\nabla} F_i(\theta_i^{k,t}), \text{ for } 0 \leq t \leq \tau - 1, \quad (2)$$

where θ_i^k denotes user i 's local model in the t -th step of the local update in round k with $\theta_i^{k,0} = \theta^k$, and $\beta > 0$

¹Different from FML, FL is a first-order method with unbiased stochastic gradients.

is the meta-learning rate. In (2), the stochastic gradient $\tilde{\nabla} F_i(\theta)$ is defined as

$$\tilde{\nabla} F_i(\theta) := (I - \alpha \tilde{\nabla}^2 f_i(\theta, \mathcal{D}_i'')) \tilde{\nabla} f_i(\theta - \alpha \tilde{\nabla} f_i(\theta, \mathcal{D}_i), \mathcal{D}_i'), \quad (3)$$

where \mathcal{D}_i , \mathcal{D}_i' and \mathcal{D}_i'' are independent batches², and for any batch \mathcal{D} , $\tilde{\nabla} f_i(\theta, \mathcal{D})$ and $\tilde{\nabla}^2 f_i(\theta, \mathcal{D})$ are the unbiased estimates of $\nabla f_i(\theta)$ and $\nabla^2 f_i(\theta)$ respectively, *i.e.*,

$$\tilde{\nabla} f_i(\theta, \mathcal{D}) := \frac{1}{|\mathcal{D}|} \sum_{(\mathbf{x}, \mathbf{y}) \in \mathcal{D}} \nabla \ell_i(\theta; \mathbf{x}, \mathbf{y}), \quad (4)$$

$$\tilde{\nabla}^2 f_i(\theta, \mathcal{D}) := \frac{1}{|\mathcal{D}|} \sum_{(\mathbf{x}, \mathbf{y}) \in \mathcal{D}} \nabla^2 \ell_i(\theta; \mathbf{x}, \mathbf{y}). \quad (5)$$

- *Global aggregation*: After updating the local model parameter, each selected user sends its local model $\theta_i^k = \theta_i^{k,\tau-1}$ back to the server. The server updates the global model by averaging over the received models, *i.e.*,

$$\theta^{k+1} = \frac{1}{n_k} \sum_{i \in \mathcal{N}_k} \theta_i^k. \quad (6)$$

It is easy to see that the main difference between federated learning and FML lies in the local update phase: In federated learning, local SGD is done using the unbiased gradient estimates while FML uses the biased one consisting of high-order information. Besides, federated learning can be considered as a special case of FML, *i.e.*, FML under $\alpha = 0$.

C. Assumptions

In this subsection, we impose the standard assumptions for the analysis of FML algorithms [10], [11], [13].

Assumption 1 (Smoothness). *The expected loss function f_i corresponding to user $i \in \mathcal{N}$ is twice continuously differentiable and L_i -smooth, *i.e.*,*

$$\|\nabla f_i(\theta_1) - \nabla f_i(\theta_2)\| \leq L_i \|\theta_1 - \theta_2\|, \quad \forall \theta_1, \theta_2 \in \mathbb{R}^d. \quad (7)$$

*Besides, its gradient is bounded by a positive constant ζ_i , *i.e.*, $\|\nabla f_i(\theta)\| \leq \zeta_i$.*

Assumption 2 (Lipschitz Hessian). *The Hessian of function f_i is ρ_i -Lipschitz continuous for each $i \in \mathcal{N}$, *i.e.*,*

$$\|\nabla^2 f_i(\theta_1) - \nabla^2 f_i(\theta_2)\| \leq \rho_i \|\theta_1 - \theta_2\|, \quad \forall \theta_1, \theta_2 \in \mathbb{R}^d. \quad (8)$$

Assumption 3 (Bounded Variance). *Given any $\theta \in \mathbb{R}^d$, the following facts hold for the stochastic gradient $\nabla \ell_i(\theta; \mathbf{x}, \mathbf{y})$ and Hessians $\nabla^2 \ell_i(\theta; \mathbf{x}, \mathbf{y})$ with $(\mathbf{x}, \mathbf{y}) \in \mathcal{X} \times \mathcal{Y}$*

$$\mathbb{E}_{(\mathbf{x}, \mathbf{y}) \sim P_i} [\nabla \ell_i(\theta; \mathbf{x}, \mathbf{y}) - \nabla f_i(\theta)] \leq \sigma_G^2, \quad (9)$$

$$\mathbb{E}_{(\mathbf{x}, \mathbf{y}) \sim P_i} [\nabla^2 \ell_i(\theta; \mathbf{x}, \mathbf{y}) - \nabla^2 f_i(\theta)] \leq \sigma_H^2. \quad (10)$$

Assumption 4 (Similarity). *For any $\theta \in \mathbb{R}^d$ and $i, j \in \mathcal{N}$, there exist nonnegative constants $\gamma_G \geq 0$ and $\gamma_H \geq 0$ such that the gradients and Hessian of the expected loss functions $f_i(\theta)$ and $f_j(\theta)$ satisfy the following conditions*

$$\|\nabla f_i(\theta) - \nabla f_j(\theta)\| \leq \gamma_G, \quad (11)$$

²We slightly abuse the notation \mathcal{D}_i as a batch of the i -th user's local dataset.

$$\|\nabla^2 f_i(\theta) - \nabla^2 f_j(\theta)\| \leq \gamma_H. \quad (12)$$

Assumption 2 implies the high-order smoothness of $f_i(\theta)$ dealing with the second-order information in the local update step (2). Assumption 4 indicates that the variations of gradients between different users are bounded by some constants, which captures the similarities between users corresponding to non-IID data. It holds for many practical loss functions [32], such as logistic regression and hyperbolic tangent functions. In particular, ψ_i^g and ψ_i^h can be roughly seen as a distance between data distributions P_i and P_j [33].

IV. NON-UNIFORM FEDERATED META-LEARNING

Due to the uniform selection of users in each round, the convergence rate of the standard FML algorithm is naturally slow. In this section, we investigate a non-uniform user selection scheme to tackle this challenge.

A. User Contribution Quantification

We begin with quantifying each user's contribution to the one-round global loss reduction using its dataset size and gradient norms. For convenience, define $\zeta := \max_i \zeta_i$, $L := \max_i L_i$, and $\rho := \max_i \rho_i$. We first provide necessary lemmas before giving the main result.

Lemma 1. *If Assumptions 1 and 2 hold, then local meta-function F_i is smooth with parameter $L_F := (1+\alpha L)^2 L + \alpha \rho \zeta$.*

Lemma 1 gives the smoothness of the local meta-function F_i and global loss function F .

Lemma 2. *Suppose that Assumptions 1-3 are satisfied, and \mathcal{D}_i , \mathcal{D}'_i , and \mathcal{D}''_i are independent batches with sizes D_i , D'_i , and D''_i respectively. Then for any $\theta \in \mathbb{R}^d$ the following holds*

$$\|\mathbb{E}[\tilde{\nabla} F_i(\theta) - \nabla F_i(\theta)]\| \leq \frac{\alpha \sigma_G L (1 + \alpha L)}{\sqrt{D_i}}, \quad (13)$$

$$\mathbb{E}[\|\tilde{\nabla} F_i(\theta) - \nabla F_i(\theta)\|^2] \leq \sigma_{F_i}^2, \quad (14)$$

where $\sigma_{F_i}^2$ is denoted as

$$\begin{aligned} \sigma_{F_i}^2 &:= 6\sigma_G^2(1 + \alpha L)^2 \left(\frac{1}{D'_i} + \frac{(\alpha L)^2}{D_i} \right) + \frac{3(\alpha \zeta \sigma_H)^2}{D''_i} \\ &\quad + \frac{6(\alpha \sigma_G \sigma_H)^2}{D''_i} \left(\frac{1}{D'_i} + \frac{(\alpha L)^2}{D_i} \right). \end{aligned} \quad (15)$$

Lemma 2 shows that the stochastic gradient $\tilde{\nabla} F_i(\theta)$ is a biased estimate of $\nabla F_i(\theta)$, revealing the challenges in analyzing FML algorithms.

Lemma 3. *If Assumptions 1, 2, and 4 are satisfied, then for any $\theta \in \mathbb{R}^d$ and $i, j \in \mathcal{N}$, we have*

$$\|\nabla F_i(\theta) - \nabla F_j(\theta)\| \leq (1 + \alpha L)^2 \gamma_G + \alpha \zeta \gamma_H. \quad (16)$$

Lemma 3 characterizes the similarities between the local meta-functions, which is critical for analyzing the one-step global loss reduction because it relates the local meta-function and global objective. Based on Lemmas 1-3, We are now ready to give our main result.

Theorem 1. *Suppose that Assumptions 1-4 are satisfied, and \mathcal{D}_i , \mathcal{D}'_i , and \mathcal{D}''_i are independent batches. If the local update and global aggregation follow (2) and (6) respectively, then the following fact holds true for $\tau = 1$*

$$\begin{aligned} \mathbb{E}[F(\theta^k) - F(\theta^{k+1})] &\geq \beta \mathbb{E} \left[\frac{1}{n_k} \sum_{i \in \mathcal{N}_k} \left(\left(1 - \frac{L_F \beta}{2}\right) \|\tilde{\nabla} F_i(\theta^k)\|^2 \right. \right. \\ &\quad \left. \left. - \left(\sqrt{(1 + \alpha L)^2 \gamma_G + \alpha \zeta \gamma_H} + \sigma_{F_i} \right) \right. \right. \\ &\quad \left. \left. \times \sqrt{\mathbb{E}[\|\tilde{\nabla} F_i(\theta^k)\|^2 | \mathcal{N}_k]} \right) \right], \end{aligned} \quad (17)$$

where the outer expectation is taken with respect to \mathcal{N}_k and data sample sizes, and the inner expectation is only regarding data sample sizes.

Theorem 1 provides a lower bound on the one-round reduction of the global objective function F based on the user selection. It quantifies each user's contribution to the objective improvement, depending on the variance of local meta-function, user similarities, smoothness, and learning rates. From Theorem 1, we have the following Corollary, which simplifies the above result and extends it to multi-step cases.

Corollary 1. *Suppose that Assumptions 1-4 are satisfied, and \mathcal{D}_i , \mathcal{D}'_i , and \mathcal{D}''_i are independent batches with $D_i = D'_i = D''_i$. If the local update and global aggregation follow (2) and (6) respectively, then the following fact holds true with $\beta \in [0, 1/L_F]$*

$$\begin{aligned} \mathbb{E}[F(\theta^k) - F(\theta^{k+1})] &\geq \frac{\beta}{2} \mathbb{E} \left[\frac{1}{n_k} \sum_{i \in \mathcal{N}_k} \sum_{t=0}^{\tau-1} \left(\|\tilde{\nabla} F_i(\theta_i^{k,t})\|^2 \right. \right. \\ &\quad \left. \left. - 2\left(\lambda_1 + \frac{\lambda_2}{\sqrt{D_i}}\right) \sqrt{\mathbb{E}[\|\tilde{\nabla} F_i(\theta_i^{k,t})\|^2 | \mathcal{N}_k]} \right) \right], \end{aligned} \quad (18)$$

where positive constants λ_1 and λ_2 satisfy that

$$\lambda_1^2 \geq ((1 + \alpha L)^2 \gamma_G + \alpha \zeta \gamma_H), \quad (19)$$

$$\begin{aligned} \lambda_2^2 &\geq 6\sigma_G^2 (1 + (\alpha L)^2) ((\alpha \sigma_H)^2 + (1 + \alpha L)^2) \\ &\quad + 3(\alpha \zeta \sigma_H)^2. \end{aligned} \quad (20)$$

Corollary 1 implies that the user with a large gradient naturally accelerates the global loss decrease, but a small dataset size would degrade the process due to corresponding high variance. Besides, as the user dissimilarities become large, the lower bound (18) weakens.

Motivated by Corollary 1, we give the user selection scheme in the following subsection.

B. User Selection

To improve the convergence speed, we aim to maximize the lower bound (18) on the one-round objective reduction. Based on Corollary 1, we define user i 's contribution u_i^k to the convergence in round k as follows

$$u_i^k := \sum_{t=0}^{\tau-1} \|\tilde{\nabla} F_i(\theta_i^{k,t})\|^2 - 2\left(\lambda_1 + \frac{\lambda_2}{\sqrt{D_i}}\right) \|\tilde{\nabla} F_i(\theta_i^{k,t})\|, \quad (21)$$

where we replace the second moment of $\tilde{\nabla}F_i(\theta_i^{k,t})$ by its sample value $\|\tilde{\nabla}F_i(\theta_i^{k,t})\|^2$. Then, the user selection problem in round k can be formulated as

$$\begin{aligned} \max_{\{z_i\}} \quad & \sum_{i \in \mathcal{N}} z_i u_i^k \\ \text{s.t.} \quad & \sum_{i \in \mathcal{N}} z_i = n_k, \\ & z_i \in \{0, 1\}, \forall i \in \mathcal{N}. \end{aligned} \quad (22)$$

Here z_i is a binary variable: $z_i = 1$ indicates selecting user i in this round; otherwise, $z_i = 0$. It is easy to see that the solution of (22) can be found by the *Select* algorithm introduced in [34, Chapter 9] with the worst-case complexity $O(n)$ (the problem (22) is indeed a *selection problem*). Accordingly, our user selection scheme is presented as follows.

User selection: Following the local update phase, instead of selecting users uniformly at random, each user i first computes its contribution scalar u_i^k locally and sends it to the server. After receiving $\{u_i^k\}_{i \in \mathcal{N}}$ from all users, the server runs the *Select* algorithm and finds the optimal user set denoted by \mathcal{N}_k^* . Notably, although λ_1 and λ_2 consist of unknown parameters such as L , γ_G , and γ_H , they can be either estimated during training as in [30] or directly tuned as in our simulations.

Based on the user selection scheme, we proposed the *Non-Uniform Federated Meta-Learning (NUFM)* algorithm (depicted in Algorithm 1). In particular, although NUFM requires an additional communication phase to upload u_i^k to the server, the communication overhead can be negligible because u_i^k is just a scalar.

V. FEDERATED META-LEARNING OVER WIRELESS NETWORKS

In this section, we extend NUFM to the context of multi-access wireless systems, where the bandwidth for uplink transmission and the power of IoT devices are limited. First, we present the system model followed by the problem formulation. Then, we decompose the original problem into two sub-problems and devise solutions for each of them with theoretical guarantees.

A. System Model

We consider a wireless multi-user system, where a set \mathcal{N} of n user devices joint forces to carry out federated meta-learning aided by an edge server. Each round consists of two stages: the computation phase and the communication phase. In the computation phase, each device $i \in \mathcal{N}$ downloads the current global model and computes the local model based on its local dataset; in the communication phase, the selected devices transmit the local models to the edge server via a limited number of wireless channels. After that, the edge server runs the global aggregation and starts the next round. Here we do not consider the downlink communication because it has a larger bandwidth than the uplink, and the edge server is also more powerful than user devices [17]. Since we focus on the user selection and resource allocation problem in each round, we omit the subscript k for brevity throughout this section.

Algorithm 1: Non-Uniform Federated Meta-Learning (NUFM)

```

Input:  $\alpha, \beta, \lambda_1, \lambda_2$ 
1 Server initializes model  $\theta^0$  and sends it to all users;
2 for round  $k = 0$  to  $K - 1$  do
3   foreach user  $i \in \mathcal{N}$  do
4     // Local update
5     Initialize  $\theta_i^{k,0} \leftarrow \theta^k$  and  $u_i^k \leftarrow 0$ ;
6     for local step  $t = 0$  to  $\tau - 1$  do
7       Compute stochastic gradient  $\tilde{\nabla}F_i(\theta_i^{k,t})$  by
8       (3) using batches  $\mathcal{D}_i$ ,  $\mathcal{D}'_i$ , and  $\mathcal{D}''_i$ ;
9       Update local model  $\theta_i^{k,t+1}$  by (2);
10      Update contribution scalar  $u_i^k$  by
11         $u_i^k \leftarrow u_i^k + \|\tilde{\nabla}F_i(\theta_i^{k,t})\|^2$ 
12         $- 2(\lambda_1 + \frac{\lambda_2}{\sqrt{D_i}})\|\tilde{\nabla}F_i(\theta_i^{k,t})\|$ ;
13    end
14    Set  $\theta_i^k = \theta_i^{k,\tau}$  and send  $u_i^k$  to server;
15  end
16  // User selection
17  Once receiving  $\{u_i^k\}_{i \in \mathcal{N}}$ , server computes optimal
18  user selection  $\mathcal{N}_k^*$  by solving (22);
19  // Global aggregation
20  After receiving local models  $\{\theta_i^k\}_{i \in \mathcal{N}_k^*}$ , server
21  computes the global model by (6);
22 end
23 return  $\theta^K$ 

```

1) *Computation Model:* We denote c_i as the CPU cycles for device i to update the model with one sample, which can be measured offline as a priori knowledge [17]. Assume that the batch size of device i used in the local update phase (2) is D_i . Then, the number of CPU cycles required for device i to run a one-step local update is $c_i D_i$. We denote the CPU-cycle frequency of device i as ν_i . Thus, the CPU energy consumption of device i in the computation during the local update phase can be expressed by

$$E_i^{cp}(\nu_i) := \frac{\iota_i}{2} \tau_i c_i D_i \nu_i^2, \quad (23)$$

where $\iota_i/2$ is the effective capacitance coefficient of device i 's computing chipset [35]. The computational time of device i in a round can be denoted as

$$T_i^{cp}(\nu_i) := \frac{\tau_i c_i D_i}{\nu_i}. \quad (24)$$

For simplicity, we set $\tau = 1$ in the following.

2) *Communication Model:* We consider a multi-access protocol for devices, *i.e.*, the orthogonal frequency division multiple access (OFDMA) technique whereby each device can occupy one uplink resource block (RB) in a communication round to upload its local model. There are M RBs in the system, denoted by $\mathcal{M} = \{1, 2, \dots, M\}$. If device i accesses RB $m \in \mathcal{M}$, the achievable transmission rate is [26]

$$r_i(z_i, p_i) := \sum_{m \in \mathcal{M}} z_{i,m} B \log_2 \left(1 + \frac{h_i p_i}{I_m + B N_0} \right), \quad (25)$$

with B being the bandwidth of each RB, h_i the channel gain, N_0 the noise power spectral density, p_i the transmission power of device i , and I_m the interference caused by the devices that are located in other service areas and use the same RB. $z_{i,m} \in \{0, 1\}$ is a binary variable giving the RB allocation for device i : $z_{i,m} = 1$ indicates that RB m is allocated to device i , and $z_{i,m} = 0$ otherwise. Each user can only occupy one RB while each RB can be accessed by at most one user, thereby it follows that

$$\sum_{m \in \mathcal{M}} z_{i,m} \leq 1 \quad \forall i \in \mathcal{N}, \quad (26)$$

$$\sum_{i \in \mathcal{N}} z_{i,m} \leq 1 \quad \forall m \in \mathcal{M}. \quad (27)$$

Due to the fixed dimension of model parameters, we assume that the model sizes of devices are constant throughout the learning process, denoted as S . If device i is selected, the time duration of transmitting the model is denoted as

$$T_i^{co}(z_i, p_i) := \frac{S}{r_i(z_i, p_i)}, \quad (28)$$

where $z_i := \{z_{i,m} \mid m \in \mathcal{M}\}$. Besides, the energy consumption of the transmission is

$$E_i^{co}(z_i, p_i) := \sum_{m \in \mathcal{M}} z_{i,m} T_i^{co}(z_i, p_i) p_i. \quad (29)$$

Naturally, if no RB is allocated to device i in current round, the transmission power and energy consumption will be zero.

B. Problem Formulation

For ease of exposition, we define $\mathbf{v} := \{v_i \mid i \in \mathcal{N}\}$, $\mathbf{p} := \{p_i \mid i \in \mathcal{N}\}$, and $\mathbf{z} := \{z_{i,m} \mid i \in \mathcal{N}, m \in \mathcal{M}\}$. Recall the procedure of NUFM. The total energy consumption $E(\mathbf{z}, \mathbf{p}, \mathbf{v})$ and wall-clock time $T(\mathbf{z}, \mathbf{p}, \mathbf{v})$ in a round can be expressed by

$$E(\mathbf{z}, \mathbf{p}, \mathbf{v}) := \sum_{i \in \mathcal{I}} \left(E_i^{cp}(v_i) + E_i^{co}(z_i, p_i) \right), \quad (30)$$

$$T(\mathbf{z}, \mathbf{p}, \mathbf{v}) := \max_{i \in \mathcal{N}} T_i^{cp}(v_i) + \max_{i \in \mathcal{N}} \sum_{m \in \mathcal{M}} z_{i,m} T_i^{co}(z_i, p_i), \quad (31)$$

where we neglect the communication time for transmitting the scalar u_i . Besides, the total contribution to the convergence is

$$U(\mathbf{z}) = \sum_{i \in \mathcal{N}} \sum_{m \in \mathcal{M}} z_{i,m} u_i, \quad (32)$$

where u_i is defined in (21)³.

We consider the following non-convex mixed-integer nonlinear programming (MINLP) problem

$$(P) \quad \max_{\mathbf{z}, \mathbf{p}, \mathbf{v}} U(\mathbf{z}) - \eta_1 E(\mathbf{z}, \mathbf{p}, \mathbf{v}) - \eta_2 T(\mathbf{z}, \mathbf{p}, \mathbf{v})$$

s.t. $0 \leq p_i \leq p_i^{max}, \forall i \in \mathcal{N},$ (33)

$$0 \leq v_i \leq v_i^{max}, \forall i \in \mathcal{N}, \quad (34)$$

$$z_{i,m} \in \{0, 1\}, \forall i \in \mathcal{N}, m \in \mathcal{M}, \quad (35)$$

$$\sum_{i \in \mathcal{N}} z_{i,m} \leq 1, \forall m \in \mathcal{M}, \quad (26)$$

$$\sum_{m \in \mathcal{M}} z_{i,m} \leq 1, \forall i \in \mathcal{N}, \quad (27)$$

³One can regularize u_i via adding a large enough constant into (21) to keep it positive.

where $\eta_1 \geq 0$ and $\eta_2 \geq 0$ are weight parameters to capture the Pareto-optimal trade-offs among convergence, latency, and energy consumption, the values of which depend on different specific scenarios. Constraints (33) and (34) give the feasible regions of devices' transmission powers and CPU-cycle frequencies, respectively. Constraints (26) and (27) restrict that each device can only access one uplink RB while each RB can be allocated to at most one device.

In this formulation, we aim to maximize the convergence speed of FML while minimizing the energy consumption and wall-clock time in each round. Notably, our solution can adapt to the problem with hard constraints on energy consumption and wall-clock time as in [16] via setting "virtual devices" (see Lemma 4 and Lemma 6).

Next, we provide a joint user selection and resource allocation algorithm to solve this problem.

C. A Joint User Selection and Resource Allocation Algorithm

Plugging (30), (31), and (32) into the problem (P), we can easily decompose the original problem into the following two sub-problems (SP1) and (SP2).

$$(SP1) \quad \min_{\mathbf{v}} \quad g_1(\mathbf{v}) = \eta_1 \sum_{i \in \mathcal{N}} \frac{\iota_i}{2} c_i D_i v_i^2 + \eta_2 \max_{i \in \mathcal{N}} \frac{c_i D_i}{v_i}$$

s.t. $0 \leq v_i \leq v_i^{max}, \forall i \in \mathcal{N}.$

$$(SP2) \quad \max_{\mathbf{z}, \mathbf{p}} \quad g_2(\mathbf{z}, \mathbf{p}) = \sum_{i \in \mathcal{N}} \sum_{m \in \mathcal{M}} z_{i,m} u_i$$

$$- \sum_{i \in \mathcal{N}} \sum_{m \in \mathcal{M}} \eta_1 \frac{S p_i}{B \log_2 \left(1 + \frac{h_i p_i}{I_m + B N_0} \right)}$$

$$- \eta_2 \max_{i \in \mathcal{N}} \sum_{m \in \mathcal{M}} z_{i,m} \frac{S}{B \log_2 \left(1 + \frac{h_i p_i}{I_m + B N_0} \right)}$$

s.t. $0 \leq p_i \leq p_i^{max}, \forall i \in \mathcal{N},$

$$\sum_{i \in \mathcal{N}} z_{i,m} \leq 1, \forall m \in \mathcal{M},$$

$$\sum_{m \in \mathcal{M}} z_{i,m} \leq 1, \forall i \in \mathcal{N},$$

$$z_{i,m} \in \{0, 1\}, \forall i \in \mathcal{N}, m \in \mathcal{M}.$$

(SP1) aims at controlling the CPU-cycle frequencies for devices to minimize the energy consumption and latency in the computational phase. (SP2) controls the transmission power and RB allocation to maximize the convergence speed while minimizing the transmission cost and communication delay. We provide the solutions to these two sub-problems separately.

1) *Solution to (SP1):* Denote the optimal CPU-cycle frequencies of (SP1) as $\mathbf{v}^* = \{v_i^* \mid i \in \mathcal{N}\}$. We first give the following lemma to offer insights into this sub-problem.

Lemma 4. *If device j is the straggler of all devices with the optimal CPU frequencies \mathbf{v}^* , i.e., $j = \arg \max_{i \in \mathcal{N}} c_i D_i / v_i^*$, then the following holds true for any $\eta_1, \eta_2 > 0$*

$$v_i^* = \begin{cases} \min \left\{ \sqrt[3]{\frac{a_2}{2a_1}}, \min_{i \in \mathcal{N}} \frac{c_j D_j v_j^{max}}{c_i D_i} \right\} & , \text{if } i = j, \\ \frac{c_i D_i v_j^*}{c_j D_j} & , \text{otherwise.} \end{cases} \quad (36)$$

The positive constants a_1 and a_2 in (36) are defined as

$$a_1 := \eta_1 \sum_{i \in \mathcal{N}} \frac{\iota_i (c_i D_i)^3}{2(c_j D_j)^2}, \quad (37)$$

$$a_2 := \eta_2 c_j D_j. \quad (38)$$

Lemma 4 implies that if the straggler (a device with the lowest computational time) can be determined, then the optimal CPU-cycle frequencies of all devices can be derived as closed-form solutions. Intuitively, due to the contradiction in minimizing the energy consumption and computational time, if the straggler is fixed, then the other devices can use the smallest CPU-cycle frequencies as long as the computational time is quicker than that of the straggler. It immediately gives the following Theorem.

Theorem 2. Denote $\mathbf{v}_{\text{straggler},j}^*$ as the optimal solution (i.e., (36)) under the assumption that j is the straggler. Then, the global optimal solution of (SP1) can be obtained by

$$\mathbf{v}^* = \arg \min_{\mathbf{v} \in \mathcal{V}} g_1(\mathbf{v}), \quad (39)$$

where $\mathcal{V} := \{\mathbf{v}_{\text{straggler},j}^*\}_{j \in \mathcal{N}}$, and g_1 is the objective function in (SP1).

Theorem 2 shows that the optimal solution of (SP1) is the fixed-straggler solution in Lemma 4 corresponding to the minimum objective g_1 . Thus, (SP1) can be solved with computational complexity $O(n)$ by comparing the achievable objective values corresponding to different stragglers.

2) *Solution to (SP2):* Similar to V-C1, we define the optimal solutions of (SP2) as $\mathbf{z}^* = \{z_{i,m}^* \mid i \in \mathcal{N}, m \in \mathcal{M}\}$ and $\mathbf{p}^* = \{p_i^* \mid i \in \mathcal{N}\}$ respectively. Besides, we denote $\mathcal{N}^* := \{i \in \mathcal{N} \mid \sum_{m \in \mathcal{M}} z_{i,m}^* = 1\}$ as the optimal set of selected devices, and for each $i \in \mathcal{N}^*$ we denote the RB block allocated to i as m_i^* , i.e., $z_{i,m_i^*}^* = 1$.

It is challenging to derive the closed-form solution for (SP2) because it is a non-convex MINLP problem with non-differentiable “max” operator in the objective. Thus, in the following we develop an iterative algorithm to solve this problem, and we also show that the algorithm will converge to a “local minimum point”.

We begin with analyzing the properties of the optimal solution in the next lemma.

Lemma 5. If we denote the transmission delay regarding \mathbf{z}^* and \mathbf{p}^* as δ^* , i.e.,

$$\delta^* := \max_{i \in \mathcal{N}} \sum_{m \in \mathcal{M}} z_{i,m}^* \frac{S}{B \log_2 \left(1 + \frac{h_i p_i^*}{I_{m_i} + BN_0} \right)}, \quad (40)$$

then the following fact holds

$$\delta^* \geq \frac{S}{B \log_2 \left(1 + \frac{h_i p_i^{\max}}{I_{m_i} + BN_0} \right)}. \quad (41)$$

Besides, p_i^* can be expressed by

$$p_i^* = \begin{cases} \frac{(I_{m_i^*} + BN_0)(2^{\frac{S}{B\delta^*}} - 1)}{h_i} & , \text{ if } i \in \mathcal{N}^*, \\ 0 & , \text{ otherwise.} \end{cases} \quad (42)$$

Lemma 5 indicates that the optimal transmission power can be derived as a closed-form via (42) given the RB allocation and transmission delay. Lemma 5 also implies that for any fixed RB allocation strategy $\tilde{\mathbf{z}}$ and transmission delay

$\tilde{\delta}$ (not necessarily optimal), the equation (42) also provides the “optimal” transmission power under $\tilde{\mathbf{z}}$ and $\tilde{\delta}$ as long as (41) is satisfied. Based on that, we have the following result.

Theorem 3. Denote $\mu_{i,m} := (I_m + BN_0)(2^{\frac{S}{B\delta^*}} - 1)/h_i$. Given transmission delay δ^* , the optimal RB allocation strategy can be obtained by

$$\mathbf{z}^* = \arg \max_{\mathbf{z}} \left\{ \sum_{i,m} z_{i,m} (u_i - e_{i,m}) , \text{ s.t. (26) - (35)} \right\}, \quad (43)$$

where $e_{i,m}$ is expressed as

$$e_{i,m} := \begin{cases} \eta_1 \delta^* \mu_{i,m} & , \text{ if } \mu_{i,m} \leq p_i^{\max}, \\ u_i + 1 & , \text{ otherwise.} \end{cases} \quad (44)$$

Theorem 3 shows the optimal RB allocation strategy can be obtained by solving (43) given fixed transmission delay δ^* . Naturally, problem (43) can be equivalently transformed to a bipartite matching problem. Consider a *Bipartite Graph* \mathcal{G} with source set \mathcal{N} and destination set \mathcal{M} . For each $i \in \mathcal{N}$ and $m \in \mathcal{M}$, denote the weight of the edge from node i to node j as $w_{i \rightarrow j}$: If $u_i - e_{i,m} > 0$, $w_{i \rightarrow j} = e_{i,m} - u_i$; otherwise, $w_{i \rightarrow j} = \infty$. Therefore, maximizing (43) is equivalent to finding a matching in \mathcal{G} with the minimum sum of weights. It means that we can obtain the optimal RB allocation strategy under fixed transmission delay via *Kuhn-Munkres* algorithm with the worst complexity of $O(Mn^2)$ [36].

We proceed to show how to iteratively approximate the optimal δ^* , \mathbf{p}^* , and \mathbf{z}^* .

Lemma 6. Let j denote the communication straggler among all selected users with respect to the RB allocation \mathbf{z}^* and transmission power \mathbf{p}^* , i.e., for any $i \in \mathcal{N}^*$

$$\begin{aligned} & \sum_{m \in \mathcal{M}} z_{i,m}^* \underbrace{\frac{S}{B \log_2 \left(1 + \frac{h_i p_i^*}{I_{m_i} + BN_0} \right)}}_{T_i^{co}(\mathbf{z}_i^*, \mathbf{p}_i^*)} \\ & \leq \sum_{m \in \mathcal{M}} z_{j,m}^* \underbrace{\frac{S}{B \log_2 \left(1 + \frac{h_j p_j^*}{I_{m_j} + BN_0} \right)}}_{T_j^{co}(\mathbf{z}_j^*, \mathbf{p}_j^*)}. \end{aligned} \quad (45)$$

Then, the following holds true

1) Define function $f_4(p) := b_1((1+p) \log_2(1+p) \ln 2 - p) - \eta_2$.

Then, $f_4(p)$ is monotonically increasing with respect to $p \geq 0$, and have unique zero point $\tilde{p}_j^0 \in (0, b_2]$, where b_1 and b_2 are denoted as follows

$$b_1 := \eta_1 \sum_{i \in \mathcal{N}^*} \frac{I_{m_i^*} + BN_0}{h_i}, \quad (46)$$

$$b_2 := 2^{(1+\sqrt{\max\{\frac{\eta_2}{b_1}, 1\}-1})/\ln 2}. \quad (47)$$

2) Denote $(SNR)_j := (I_{m_j^*} + BN_0)/h_j$. For $i \in \mathcal{N}^*$, we have

$$p_i^* = \begin{cases} \min \left\{ \tilde{p}_j^0, \min_{i \in \mathcal{N}^*} \frac{h_i p_i^{\max}}{I_{m_i^*} + BN_0} \right\} & , \text{ if } i = j, \\ \frac{(SNR)_i}{(SNR)_j} p_j^* & , \text{ otherwise.} \end{cases} \quad (48)$$

Algorithm 2: Iterative Solution (IVES)

Input: $\eta_1, \eta_2, S, B, \{h_i\}, \{I_m\}$.
1 Initialize $t = 0$ and δ_0 by (50);
2 **while** not done **do**
3 Compute RB allocation strategy z^t under δ^t using Kuhn-Munkres algorithm based on (43);
4 Compute transmission power p^t by (49);
5 Update $\delta^{t+1} = T^{co}(z^t, p^t)$;
6 **end**
7 **return** z^*, p^*

Lemma 6 indicates that given the optimal RB allocation strategy z^* and straggler, the optimal transmission power can be derived by (48) (different from Lemma 5 that requires the corresponding transmission delay δ^*). Notably, in (48), we can easily obtain the zero point \tilde{p}_j^0 of f_4 with any required tolerance ϵ by *Bisection method* in at most $\log_2(\frac{b_2}{\epsilon})$ iterations.

Similar to Theorem 2, we can find the optimal transmission power by the following theorem given the RB allocation.

Theorem 4. Denote $p_{\text{straggler},j}^*$ as the optimal solution under the assumption that j is the communication straggler under fixed RB allocation z^* . The corresponding optimal transmission power can be expressed by

$$p^* = \arg \max_{p \in \mathcal{P}} g_2(z^*, p), \quad (49)$$

where $\mathcal{P} := \{p_{\text{straggler},j}^*\}_{j \in N}$ and g_2 is the objective function defined in (SP2).

Define the communication time corresponding to z and p as $T^{co}(z, p) := \max_{i \in N} \sum_{m \in M} z_{i,m} T_i^{co}(z_i, p_i)$. Based on Theorem 3 and 4, we give the following *Iterative Solution (IVES)* to solve (SP2).

IVES: We initialize transmission delay δ^0 (based on (42)) as follows

$$\delta^0 = \max_{i \in N} \frac{S}{B \log_2 \left(1 + \frac{h_i p_i^{\max}}{I_m + BN_0} \right)}. \quad (50)$$

In each iteration t , we first compute an RB allocation strategy z^t via solving (43) by the *Kuhn-Munkres* algorithm. Then, based on z^t , we find the corresponding transmission power p^t by (49) and update the transmission delay by $\delta^{t+1} = T^{co}(z^t, p^t)$ before the next iteration. The details of IVES are depicted in Algorithm 2.

Using IVES, we can solve (SP2) in an iterative manner. In the following theorem, we provide the convergence guarantee for IVES.

Theorem 5. If we solve (SP2) by IVES, then $\{g_2(z^t, p^t)\}$ is monotonically increasing and converges to a unique point.

It is worth noting that although IVES solves (SP2) iteratively, we find it converges extremely fast (often with only two iterations) in the simulation. Thus, we expect IVES can achieve a low computation complexity in practice.

Combining the solutions of (SP1) and (SP2), we provide the *User selection and Resource Allocation (URAL)* in Algorithm

Algorithm 3: User Selection and Resource Allocation (URAL) Algorithm

Input: $\eta_1, \eta_2, S, B, \{h_i\}, \{I_m\}, \{\iota_i\}, \{c_i\}, \{D_i\}$.
1 Compute v^* by (39); // Solve (SP1)
2 Compute z^* and p^* by IVES; // Solve (SP2)
3 **return** v^*, z^*, p^*

3 to solve the original problem (P). URAL can simultaneously optimize the convergence speed, training time, and energy consumption via jointly selecting devices and allocating resources. Besides, URAL can be directly integrated into the NUFM paradigm in the user selection phase to facilitate the deployment of FML in today's wireless networks.

VI. EXTENSION TO FIRST-ORDER APPROXIMATIONS

Due to the computation of Hessian in the local update (2), it may cause high computational cost for resource-limited IoT devices. In this section, we attempt to address this challenge.

There are two common methods used in the literature to reduce the complexity in computing Hessian [11]:

1) Replacing the stochastic gradient by

$$\tilde{\nabla}F_i(\theta) \approx \tilde{\nabla}f_i(\theta - \alpha \tilde{\nabla}f_i(\theta, \mathcal{D}_i), \mathcal{D}'_i); \quad (51)$$

2) Replacing the Hessian-gradient product by

$$\begin{aligned} \tilde{\nabla}^2 f_i(\theta, \mathcal{D}'_i) \tilde{\nabla} f_i(\theta - \alpha \tilde{\nabla} f_i(\theta, \mathcal{D}_i), \mathcal{D}'_i) \\ \approx \frac{\tilde{\nabla} f_i(\theta + \epsilon \tilde{g}_i, \mathcal{D}'_i) - \tilde{\nabla} f_i(\theta - \epsilon \tilde{g}_i, \mathcal{D}'_i)}{\epsilon}, \end{aligned} \quad (52)$$

$$\text{where } \tilde{g}_i = \tilde{\nabla} f_i(\theta - \alpha \tilde{\nabla} f_i(\theta, \mathcal{D}_i), \mathcal{D}'_i).$$

By doing so, the computational complexity of a one-step local update can be reduced from $O(d^2)$ to $O(d)$ while it will not sacrifice too much learning performance. Next, we show that our results in Theorem 1 still hold in the above two cases.

Corollary 2. Suppose that Assumptions 1-4 are satisfied, and \mathcal{D}_i , \mathcal{D}'_i , and \mathcal{D}''_i are independent batches. If the local update and global aggregation follow (2) and (6) respectively, then the following fact holds true for $\tau = 1$

$$\begin{aligned} \mathbb{E}[F(\theta^k) - F(\theta^{k+1})] &\geq \beta \mathbb{E} \left[\frac{1}{n_k} \sum_{i \in N_k} \left(\left(1 - \frac{L_F \beta}{2} \right) \|\tilde{\nabla}F_i(\theta^k)\|^2 \right. \right. \\ &\quad \left. \left. - \left(\sqrt{(1 + \alpha L)^2 \gamma_G + \alpha \zeta \gamma_H} + \tilde{\sigma}_{F_i} \right) \right. \right. \\ &\quad \left. \left. \times \sqrt{\mathbb{E}[\|\tilde{\nabla}F_i(\theta^k)\|^2 | \mathcal{N}_k]} \right) \right], \end{aligned} \quad (53)$$

where $\tilde{\sigma}_{F_i}$ is defined as follows

$$\tilde{\sigma}_{F_i}^2 = \begin{cases} 2\sigma_G^2 \left(\frac{1}{D'} + \frac{(\alpha L)^2}{D} \right) + 2(\alpha LB)^2 & , \text{ if using (51),} \\ 6\sigma_G^2 \left(\frac{2(\alpha L)^2}{D} + \frac{2}{D'} + \frac{\alpha^2}{2\epsilon^2 D''} \right) + 2(\alpha \mu \delta)^2 \zeta^4 & , \text{ if using (52).} \end{cases} \quad (54)$$

Corollary 2 indicates that NUFM can be directly combined with the first-order approximation techniques to reduce computational cost. Further, similar to Corollary 1, Corollary 2 can be easily extended to the multi-step cases.

VII. SIMULATION

This section evaluates the performance of our proposed algorithms by comparing with existing baselines in real-world datasets. We first present the experimental setup, including the datasets, models, parameters, baselines, and environment. Then we provide our results from various aspects.

A. Experimental Setup

1) *Datasets and Models*: We evaluate our algorithms on four widely-used benchmarks, namely Fashion-MNIST [37], CIFAR-10 [38], CIFAR-100 [38], and ImageNet [39]. Specifically, the data is distributed among $n = 100$ devices as follows: a) Each device has samples from two random classes; b) the number of samples per class follows a truncated Gaussian distribution $\mathcal{N}(\mu, \sigma^2)$ with $\mu = 5$ and $\sigma = 5$. We select 50% devices at random for training with the rest for testing. For each device, we divide the local dataset into a support set and a query set. We consider 1-shot 2-class classification tasks, *i.e.*, the support set contains only 1 labeled example for each class. We set the stepsizes as $\alpha = \beta = 0.001$. We use a convolutional neural network (CNN) with max-pooling operations and the Leaky Rectified Linear Unit (Leaky ReLU) activation function, containing three convolutional layers with sizes 32, 64, and 128 followed by a fully connected layer and a softmax layer. The strides are set as 1 for convolution operation and 2 for the pooling operation.

2) *Baselines*: To compare the performance of NUFM, we first consider two existing algorithms, *i.e.*, FedAvg [5] and Per-FedAvg [11]. Further, to validate the effectiveness of URAL in the multi-access wireless networks, we use two baselines, called *Greedy* and *Random*. In each round, the *Greedy* strategy determines the CPU-cycle frequency v_i^g and transmission power p_i^g for the device $i \in \mathcal{N}$ by greedily minimizing its personal objective, *i.e.*,

$$v_i^g = \arg \min_{v_i} \left\{ \eta_1 \frac{\iota_i c_i D_i v_i^2}{2} + \eta_2 \frac{c_i D_i}{v_i}, \text{ s.t. (34)} \right\}, \quad (55)$$

$$p_i^g = \arg \min_{p_i} \left\{ \sum_{m \in \mathcal{M}} \frac{z_{i,m}^g (\eta_1 p_i + \eta_2) S}{B \log_2 \left(\frac{1+h_i p_i}{I_m + B N_0} \right)}, \text{ s.t. (33)} \right\}, \quad (56)$$

where $\{z_{i,m}^g\}_{m \in \mathcal{M}}$ is selected at random (*i.e.*, randomly allocating RBs to selected devices). The *Random* strategy just decides the CPU-cycle frequencies, transmission powers, and RB allocation for the selected users uniformly at random from the feasible regions.

3) *Implementation*: We implement the code in TensorFlow Version 1.14 on a server with two Intel® Xeon® Golden 5120 CPUs and one Nvidia® Tesla-V100 32G GPU.

B. Experimental Results

1) *Convergence Speed*: To demonstrate the improvement of NUFM on the convergence speed, we compare the algorithms on different benchmarks with the same initial model and learning rate. We vary the number of participated devices n_k from 20 to 40, and set the numbers of local update steps and total communication rounds as $\tau = 1$ and $K = 50$, respectively.

We let $\lambda_1 = \lambda_2 = 1$. As illustrated in Fig. 1 and Table VII-B1, NUFM significantly improve the convergence speed and corresponding test accuracy of the existing FML approach on all datasets. Clearly, it validates the effectiveness of our proposed user selection scheme that principally maximizes the lower bound of one-round global loss reduction. Interestingly, Fig. 1 also indicates that NUFM converges more quickly with relatively fewer participated devices. For example, in the round 19, the loss achieved by NUFM with $n_k = 20$ decreases by more than 9% and 20% over those with $n_k = 30$ and $n_k = 40$ on Fashion-MNIST, respectively. The underlying rationale is that relatively fewer “good” devices can provide a larger lower bound on the one-round global loss decrease (note that in (17) the lower bound takes the average of the selected devices). Naturally, more selected devices in each round generally require more communication resources. Thus, the results reveal the potential of NUFM in being applied to resource-limited wireless systems.

TABLE I
TEST ACCURACY AFTER FIFTY ROUNDS OF TRAINING.

Algorithm	Fashion-MNIST	CIFAR-10	CIFAR-100	ImageNet
NUFM	68.04%	58.80%	23.95%	34.04%
Per-FedAvg	62.75%	58.22%	21.49%	30.98%
FedAvg	61.04%	54.31%	10.13%	12.14%

2) *Effect of Local Update Steps*: To show the effect of local update steps on the convergence rate of NUFM, we present results with varying numbers of local update steps in each round. For ease of illustration, we compare the loss under different numbers of local steps in the round 19 on Fashion-MNIST and CIFAR-100. Fig. 2 shows that fewer local update steps lead to a larger gap between the baselines and NUFM, which verifies the theoretical result that a small number of local steps would slow the convergence of FedAvg and Per-FedAvg [11, Theorem 4.5]. It also implies that NUFM can improve the computational efficiency of local devices.

3) *Performance of URAL in wireless networks*: We evaluate the performance of URAL by comparing with four baselines, namely NUFM-*Greedy*, NUFM-*Random*, RU-*Greedy*, and RU-*Random*, which are defined below.

- NUFM-*Greedy*: select devices by NUFM; decide CPU-cycle frequencies, RB allocation, and transmission power by *Greedy* strategy.
- NUFM-*Random*: select devices by NUFM; decide CPU-cycle frequencies, RB allocation, and transmission power by *Random* strategy.
- RU-*Greedy*: select devices uniformly at random; decide CPU-cycle frequencies, RB allocation, and transmission power by *Greedy* strategy.
- RU-*Random*: select devices uniformly at random; decide CPU-cycle frequencies, RB allocation, and transmission power by *Random* strategy.

We simulate a wireless system consisting of $M = 20$ RBs and let the channel gain h_i of each device i follow a uniform distribution $U(h^{\min}, h^{\max})$ with $h^{\min} = 0.1$ and $h^{\max} = 1$. The interference of RB m is drawn from $I_m \sim U(0, 0.8)$. We set $p_i^{\max} \sim U(0, 1)$ and $v_i^{\max} \sim U(0, 2)$ for each $i \in \mathcal{N}$ to simulate

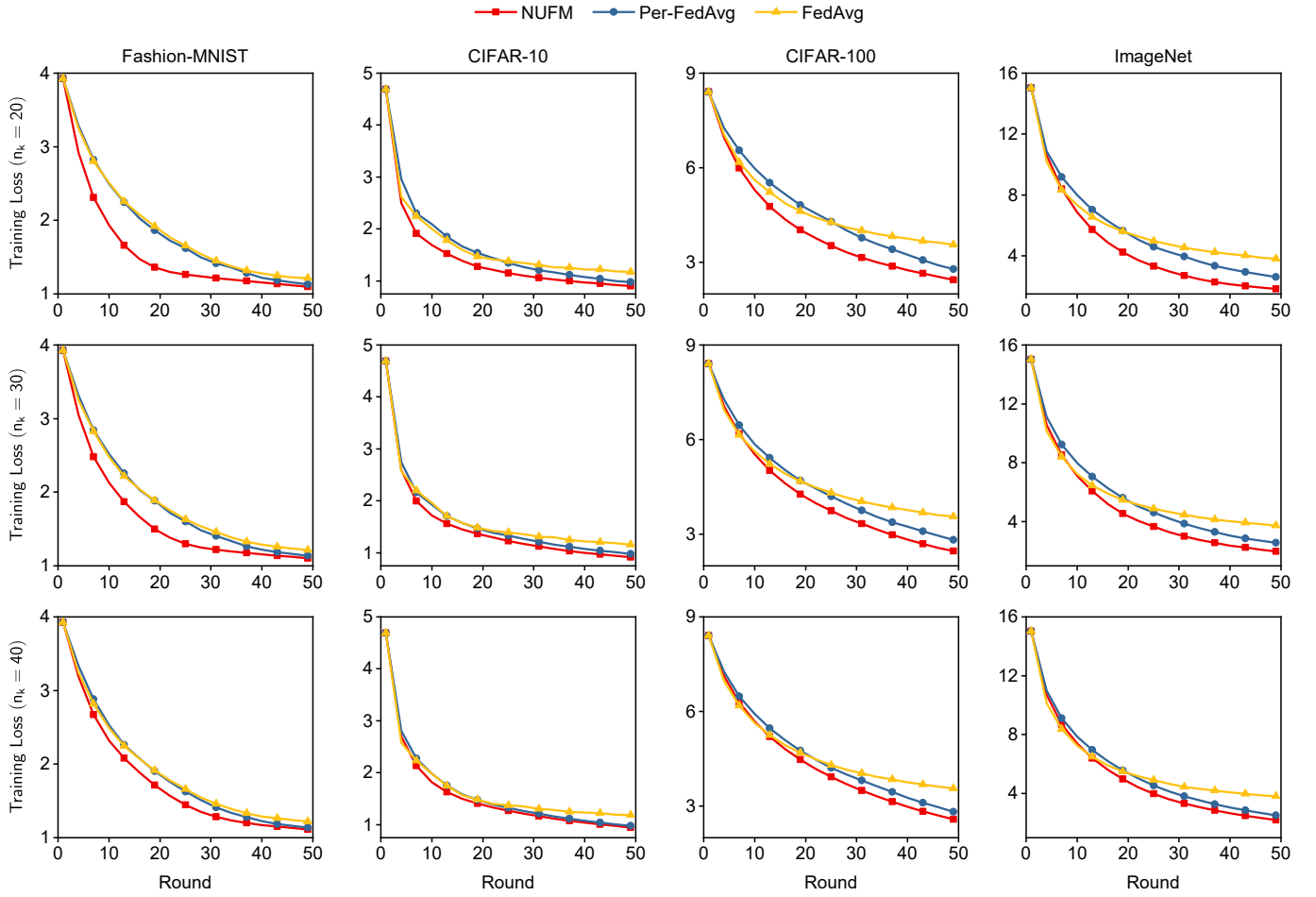


Fig. 1. Comparison of convergence rates under different numbers of participated devices. NUFM significantly accelerates the convergence of the existing FML approach, especially with fewer participated devices.

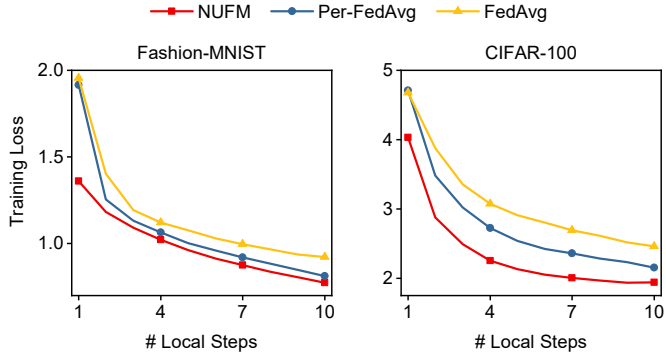


Fig. 2. Effect of local update steps on convergence rates. Fewer local steps lead to larger gaps between NUFM and the existing methods.

the device heterogeneity. In the following experiments, we run the algorithms on FMNIST with local update steps $\tau = 1$ and $\eta_1 = \eta_2 = 1$.

As shown in Fig. 3, URAL can significantly reduce energy consumption and wall-clock time compared with the baselines. However, it is counter-intuitive that the *Greedy* strategy is not always better than *Random*. There are two reasons. On the one hand, the energy cost and wall-clock time depend on the selection of the weight parameters η_1 and η_2 . The results in Fig. 3 imply that when $\eta_1 = \eta_2 = 1$, *Greedy* pays more

attention to the wall-clock time rather than energy consumption. Accordingly, *Greedy* achieves much lower average delay than that of *Random* but sacrificing parts of the energy. On the other hand, the wall-clock time and energy cost require controlling jointly with the RB allocation strategy. Although *Greedy* minimizes the personal objectives (55)-(56), improper RB allocation would cause arbitrary performance degradation. Unlike *Greedy* and *Random*-based baselines, since URAL aims to maximize the joint objective (P) via co-optimizing the CPU-cycle frequencies, transmission power, and RB allocation strategy, it can alleviate the above-mentioned issues, and achieve a better delay and energy control. At the same time, Fig. 3 also indicates that URAL converges as fast as NUFM-*Greedy* and NUFM-*Random* (the corresponding lines are almost overlapped), which select devices greedily to accelerate convergence (as in NUFM). Thus, URAL can also provide an excellent convergence rate.

4) *Effect of Resource Blocks:* In Fig. 4, we test the performance of URAL under different numbers of RBs. We vary the number of RBs M from 1 to 50. More RBs enable more devices to be selected in each round, naturally leading to larger energy consumption. As shown in Fig. 4, URAL keeps stable wall-clock time with the increase of RBs. Meanwhile, URAL can also well control the power in devices to avoid serious waste of energy. It is counter-intuitive that the convergence

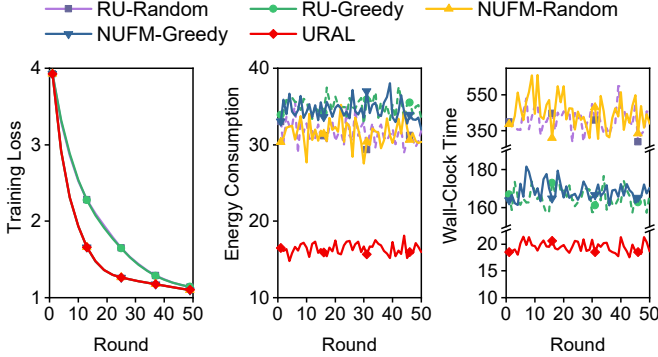


Fig. 3. Comparison of convergence, energy cost, and wall-clock training time. URAL can achieve a great convergence speed and short wall-clock time with low energy consumption.

speed is not always decreasing with the increase of RBs, especially for URAL. The reason is indeed the same as that in VII-B1. That is, too few selected devices would slow the convergence due to insufficient information provided in each round while a large number of participated devices may weaken the global loss reduction as shown in (1). Therefore, URAL can well adapt to the practical systems with constrained wireless resources because it can achieve fast convergence with only a small set of devices.

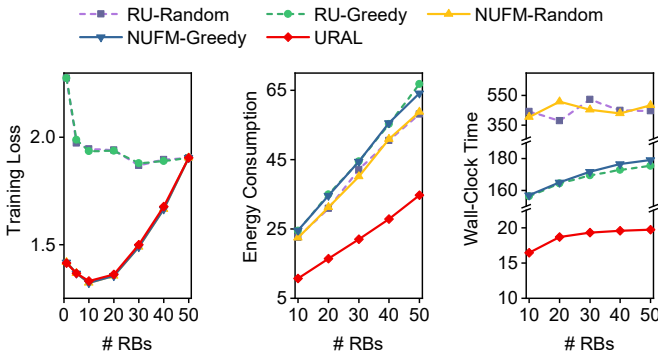


Fig. 4. Comparison of convergence, energy cost, and wall-clock time under different numbers of RBs. URAL can well control the energy cost and wall-clock time with more available RBs. Meanwhile, it can achieve fast convergence with only a small number of RBs.

5) *Effect of Channel Quality*: To investigate the effect of channel conditions on performance, we fix the number of RBs $M = 20$ and vary the maximum channel gain h^{max} from 0.25 to 2 and show the corresponding energy consumption and wall-clock training time in Fig. 5. The results indicate that the energy consumption and latency would decrease as channel quality improves, because devices can use less power to achieve a relatively large transmission rate.

6) *Effect of Weight Parameters*: We study how the weight parameters η_1 and η_2 affect the average energy consumption and wall-clock time of URAL in Fig. 6. We first fix $\eta_2 = 1$ and vary η_1 from 0.5 to 2.5. As expected, we find the total energy consumption decreases with the increase of η_1 while the wall-clock time is the opposite. Then we vary η_2 with fixed $\eta_1 = 1$. Similarly, a larger η_2 leads to less latency and more energy cost. It implies that we can control the levels of wall-clock training time and energy consumption by tuning

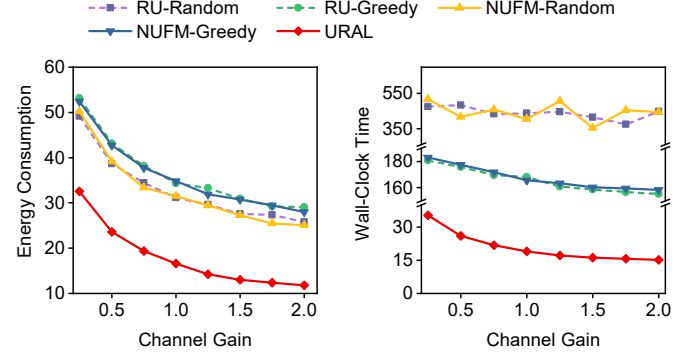


Fig. 5. Effect of channel gains on performance. Worse channel conditions would induce larger transmission power and longer wall-clock time.

the weight parameters. In particular, even with a large η_1 or η_2 , the wall-clock time and energy cost are still controlled in low levels. Meanwhile, the convergence rate achieved by URAL is robust to η_1 and η_2 . Thus, URAL can take full use of the resources (including datasets, bandwidth, and power) and achieve great trade-offs among the convergence rate, latency, and energy consumption.

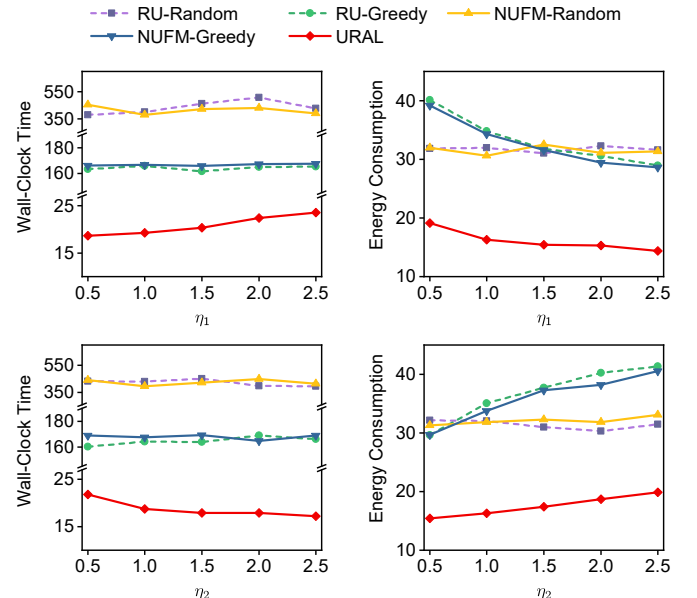


Fig. 6. Effect of weight parameters η_1 and η_2 . A large η_1 achieves lower energy consumption while leading to longer wall-clock time (the average wall-clock time is 18.63 when $\eta_1 = 0.5$; it is 21.53 when $\eta_1 = 2.5$). It is the opposite for η_2 .

VIII. CONCLUSION

In this paper, we provided an FML algorithm, called NUFM, that maximizes the theoretical lower bound of global loss reduction in each round to accelerate the convergence. Aiming at deploying NUFM in wireless networks effectively, we then devised a user selection and resource allocation strategy (URAL), which jointly controls the CPU-cycle frequencies and RB allocation to optimize the trade-off between energy consumption and wall-clock training time. Moreover, we integrated the proposed algorithms with two first-order approximation techniques to further reduce the computational complexity

in IoT devices. Extensive simulation results demonstrated that the proposed methods outperform the baseline algorithms.

Future work can consider the trade-off between the local update and global aggregation in FML to minimize the convergence time and energy cost from a long-term perspective. Besides, it is intriguing to characterize the convergence properties and communication complexity of the NUFM algorithm.

REFERENCES

- [1] J. Park, S. Samarakoon, M. Bennis, and M. Debbah, "Wireless network intelligence at the edge," *Proceedings of the IEEE*, vol. 107, no. 11, pp. 2204–2239, 2019.
- [2] Z. Zhou, X. Chen, E. Li, L. Zeng, K. Luo, and J. Zhang, "Edge intelligence: Paving the last mile of artificial intelligence with edge computing," *Proceedings of the IEEE*, vol. 107, no. 8, pp. 1738–1762, 2019.
- [3] G. Plastiras, M. Terzi, C. Kyrou, and T. Theοcharidcs, "Edge intelligence: Challenges and opportunities of near-sensor machine learning applications," in *2018 ieee 29th international conference on application-specific systems, architectures and processors (asap)*. IEEE, 2018, pp. 1–7.
- [4] X. Zhang, Y. Wang, S. Lu, L. Liu, W. Shi *et al.*, "Openei: An open framework for edge intelligence," in *2019 IEEE 39th International Conference on Distributed Computing Systems (ICDCS)*. IEEE, 2019, pp. 1840–1851.
- [5] B. McMahan, E. Moore, D. Ramage, S. Hampson, and B. A. y Arcas, "Communication-efficient learning of deep networks from decentralized data," in *Artificial intelligence and statistics*. PMLR, 2017, pp. 1273–1282.
- [6] C. Finn, P. Abbeel, and S. Levine, "Model-agnostic meta-learning for fast adaptation of deep networks," in *International Conference on Machine Learning*. PMLR, 2017, pp. 1126–1135.
- [7] A. Nichol, J. Achiam, and J. Schulman, "On first-order meta-learning algorithms," *arXiv preprint arXiv:1803.02999*, 2018.
- [8] F. Chen, M. Luo, Z. Dong, Z. Li, and X. He, "Federated meta-learning with fast convergence and efficient communication," *arXiv preprint arXiv:1802.07876*, 2018.
- [9] Y. Jiang, J. Konečný, K. Rush, and S. Kannan, "Improving federated learning personalization via model agnostic meta learning," *arXiv preprint arXiv:1909.12488*, 2019.
- [10] S. Lin, G. Yang, and J. Zhang, "A collaborative learning framework via federated meta-learning," in *2020 IEEE 40th International Conference on Distributed Computing Systems (ICDCS)*. IEEE Computer Society, 2020, pp. 289–299.
- [11] A. Fallah, A. Mokhtari, and A. Ozdaglar, "Personalized federated learning with theoretical guarantees: A model-agnostic meta-learning approach," *Advances in Neural Information Processing Systems*, vol. 33, 2020.
- [12] P. Kairouz, H. B. McMahan, B. Avent, A. Bellet, M. Bennis, A. N. Bhagoji, K. Bonawitz, Z. Charles, G. Cormode, R. Cummings *et al.*, "Advances and open problems in federated learning," *arXiv preprint arXiv:1912.04977*, 2019.
- [13] S. Yue, J. Ren, J. Xin, S. Lin, and J. Zhang, "Inexact-admm based federated meta-learning for fast and continual edge learning," in *Proceedings of the Twenty-Second International Symposium on Theory, Algorithmic Foundations, and Protocol Design for Mobile Networks and Mobile Computing*, ser. MobiHoc '21. New York, NY, USA: Association for Computing Machinery, 2021, p. 91–100. [Online]. Available: <https://doi.org/10.1145/3466772.3467038>
- [14] T. Nishio and R. Yonetani, "Client selection for federated learning with heterogeneous resources in mobile edge," in *ICC 2019-2019 IEEE International Conference on Communications (ICC)*. IEEE, 2019, pp. 1–7.
- [15] H. T. Nguyen, V. Sehwag, S. Hosseinalipour, C. G. Brinton, M. Chiang, and H. V. Poor, "Fast-convergent federated learning," *IEEE Journal on Selected Areas in Communications*, vol. 39, no. 1, pp. 201–218, 2020.
- [16] M. Chen, Z. Yang, W. Saad, C. Yin, H. V. Poor, and S. Cui, "A joint learning and communications framework for federated learning over wireless networks," *IEEE Transactions on Wireless Communications*, vol. 20, no. 1, pp. 269–283, 2020.
- [17] C. T. Dinh, N. H. Tran, M. N. Nguyen, C. S. Hong, W. Bao, A. Y. Zomaya, and V. Gramoli, "Federated learning over wireless networks: Convergence analysis and resource allocation," *IEEE/ACM Transactions on Networking*, vol. 29, no. 1, pp. 398–409, 2020.
- [18] Q. Wu, K. He, and X. Chen, "Personalized federated learning for intelligent iot applications: A cloud-edge based framework," *IEEE Open Journal of the Computer Society*, vol. 1, pp. 35–44, 2020.
- [19] Q. Yang, Y. Liu, T. Chen, and Y. Tong, "Federated machine learning: Concept and applications," *ACM Transactions on Intelligent Systems and Technology (TIST)*, vol. 10, no. 2, pp. 1–19, 2019.
- [20] J. Li, M. Khodak, S. Caldas, and A. Talwalkar, "Differentially private meta-learning," in *International Conference on Learning Representations*, 2019.
- [21] K. C. Sim, F. Beaufays, A. Benard, D. Guliani, A. Kabel, N. Khare, T. Lucassen, P. Zadrazil, H. Zhang, L. Johnson *et al.*, "Personalization of end-to-end speech recognition on mobile devices for named entities," in *2019 IEEE Automatic Speech Recognition and Understanding Workshop (ASRU)*. IEEE, 2019, pp. 23–30.
- [22] J. Ren, Y. He, D. Wen, G. Yu, K. Huang, and D. Guo, "Scheduling for cellular federated edge learning with importance and channel awareness," *IEEE Transactions on Wireless Communications*, vol. 19, no. 11, pp. 7690–7703, 2020.
- [23] G. Zhu, Y. Wang, and K. Huang, "Broadband analog aggregation for low-latency federated edge learning," *IEEE Transactions on Wireless Communications*, vol. 19, no. 1, pp. 491–506, 2019.
- [24] Q. Zeng, Y. Du, K. Huang, and K. K. Leung, "Energy-efficient radio resource allocation for federated edge learning," in *2020 IEEE International Conference on Communications Workshops (ICC Workshops)*. IEEE, 2020, pp. 1–6.
- [25] W. Shi, S. Zhou, Z. Niu, M. Jiang, and L. Geng, "Joint device scheduling and resource allocation for latency constrained wireless federated learning," *IEEE Transactions on Wireless Communications*, vol. 20, no. 1, pp. 453–467, 2020.
- [26] M. Chen, H. V. Poor, W. Saad, and S. Cui, "Convergence time optimization for federated learning over wireless networks," *IEEE Transactions on Wireless Communications*, vol. 20, no. 4, pp. 2457–2471, 2020.
- [27] J. Ren, G. Yu, and G. Ding, "Accelerating dnn training in wireless federated edge learning systems," *IEEE Journal on Selected Areas in Communications*, vol. 39, no. 1, pp. 219–232, 2020.
- [28] H. Yu, R. Jin, and S. Yang, "On the linear speedup analysis of communication efficient momentum sgd for distributed non-convex optimization," in *International Conference on Machine Learning*. PMLR, 2019, pp. 7184–7193.
- [29] J. Xu and H. Wang, "Client selection and bandwidth allocation in wireless federated learning networks: A long-term perspective," *IEEE Transactions on Wireless Communications*, vol. 20, no. 2, pp. 1188–1200, 2020.
- [30] S. Wang, T. Tuor, T. Salonidis, K. K. Leung, C. Makaya, T. He, and K. Chan, "Adaptive federated learning in resource constrained edge computing systems," *IEEE Journal on Selected Areas in Communications*, vol. 37, no. 6, pp. 1205–1221, 2019.
- [31] S. P. Karimireddy, S. Kale, M. Mohri, S. Reddi, S. Stich, and A. T. Suresh, "Scaffold: Stochastic controlled averaging for federated learning," in *International Conference on Machine Learning*. PMLR, 2020, pp. 5132–5143.
- [32] X. Zhang, M. Hong, S. V. Dhople, W. Yin, and Y. Liu, "Fedpd: A federated learning framework with optimal rates and adaptivity to non-iid data," *CoRR*, vol. abs/2005.11418, 2020. [Online]. Available: <https://arxiv.org/abs/2005.11418>
- [33] A. Fallah, A. Mokhtari, and A. Ozdaglar, "On the convergence theory of gradient-based model-agnostic meta-learning algorithms," in *International Conference on Artificial Intelligence and Statistics*. PMLR, 2020, pp. 1082–1092.
- [34] T. H. Cormen, C. E. Leiserson, R. L. Rivest, and C. Stein, *Introduction to algorithms*. MIT press, 2009.
- [35] T. D. Burd and R. W. Brodersen, "Processor design for portable systems," *Journal of VLSI signal processing systems for signal, image and video technology*, vol. 13, no. 2, pp. 203–221, 1996.
- [36] E. W. Weisstein, "Hungarian maximum matching algorithm," <https://mathworld.wolfram.com/>, 2011.
- [37] H. Xiao, K. Rasul, and R. Vollgraf, "Fashion-mnist: a novel image dataset for benchmarking machine learning algorithms," *arXiv preprint arXiv:1708.07747*, 2017.
- [38] A. Krizhevsky *et al.*, "Learning multiple layers of features from tiny images," 2009.
- [39] J. Deng, W. Dong, R. Socher, L.-J. Li, K. Li, and L. Fei-Fei, "Imagenet: A large-scale hierarchical image database," in *2009 IEEE conference on computer vision and pattern recognition*. Ieee, 2009, pp. 248–255.

APPENDIX A
PROOF OF LEMMA 1

The proof is standard [11], [13], and we provide it for completeness. First, for any $\theta_1, \theta_2 \in \mathbb{R}^d$ we have

$$\begin{aligned}
 \|\nabla F_i(\theta_1) - \nabla F_i(\theta_2)\| &= \|(I - \alpha \nabla^2 f_i(\theta_1)) \nabla f_i(\theta_1 - \alpha \nabla f_i(\theta_1)) - (I - \alpha \nabla^2 f_i(\theta_2)) \nabla f_i(\theta_2 - \alpha \nabla f_i(\theta_2))\| \\
 &= \|(I - \alpha \nabla^2 f_i(\theta_1))(\nabla f_i(\theta_1 - \alpha \nabla f_i(\theta_1)) - \nabla f_i(\theta_2 - \alpha \nabla f_i(\theta_2))) \\
 &\quad + ((I - \alpha \nabla^2 f_i(\theta_1)) - (I - \alpha \nabla^2 f_i(\theta_2))) \nabla f_i(\theta_2 - \alpha \nabla f_i(\theta_2))\| \\
 &\leq \underbrace{\|I - \alpha \nabla^2 f_i(\theta_1)\| \|\nabla f_i(\theta_1 - \alpha \nabla f_i(\theta_1)) - \nabla f_i(\theta_2 - \alpha \nabla f_i(\theta_2))\|}_{(a)} \quad (\text{from triangle inequality}) \\
 &\quad + \underbrace{\alpha \|\nabla^2 f_i(\theta_1) - \nabla^2 f_i(\theta_2)\| \|\nabla f_i(\theta_2 - \alpha \nabla f_i(\theta_2))\|}_{(b)}. \tag{57}
 \end{aligned}$$

Then, for (a), the following holds true

$$\begin{aligned}
 &\|I - \alpha \nabla^2 f_i(\theta_1)\| \|\nabla f_i(\theta_1 - \alpha \nabla f_i(\theta_1)) - \nabla f_i(\theta_2 - \alpha \nabla f_i(\theta_2))\| \\
 &\leq (1 + \alpha L) L \|\theta_1 - \alpha \nabla f_i(\theta_1) - \theta_2 + \alpha \nabla f_i(\theta_2)\| \quad (\text{from Assumption 1}) \\
 &\leq (1 + \alpha L) L (\|\theta_1 - \theta_2\| + \alpha \|\nabla f_i(\theta_1) - \nabla f_i(\theta_2)\|) \quad (\text{from triangle inequality}) \\
 &\leq (1 + \alpha L)^2 L \|\theta_1 - \theta_2\|. \tag{58}
 \end{aligned}$$

Regarding (b), it can be easily shown that

$$\|\nabla^2 f_i(\theta_1) - \nabla^2 f_i(\theta_2)\| \|\nabla f_i(\theta_2 - \alpha \nabla f_i(\theta_2))\| \leq \rho \zeta \|\theta_1 - \theta_2\|. \quad (\text{from Assumptions 1 and 2})$$

Plugging (a) and (b) into (57), we give the result.

APPENDIX B
PROOF OF LEMMA 2

We provide this proof for completeness. The proof is essentially the same as that for [11, Lemma].

We rewrite the stochastic gradient $\tilde{\nabla} F_i(\theta)$ as follows

$$\tilde{\nabla} F_i(\theta) = \left(I - \alpha \nabla^2 f_i(\theta) + \delta_1^* \right) (\nabla f_i(\theta - \alpha \nabla f_i(\theta)) + \delta_2^*), \tag{59}$$

where δ_1^* and δ_2^* are denoted as

$$\delta_1^* = \alpha \left(\nabla^2 f_i(\theta) - \tilde{\nabla}^2 f_i(\theta, \mathcal{D}_i'') \right), \tag{60}$$

$$\delta_2^* = \tilde{\nabla} f_i(\theta - \alpha \tilde{\nabla} f_i(\theta, \mathcal{D}_i), \mathcal{D}_i') - \nabla f_i(\theta - \alpha \nabla f_i(\theta)). \tag{61}$$

Note that δ_1^* and δ_2^* are independent. Due to Assumption 3, the first and second moments of δ_1^* can be bounded by

$$\mathbb{E}[\delta_1^*] = 0 \tag{62}$$

$$\mathbb{E}[\|\delta_1^*\|^2] \leq \frac{(\alpha \sigma_H)^2}{D_i''}. \tag{63}$$

Next, we proceed to bound the first and second moments of δ_2^* . Regarding the first moment, we have

$$\begin{aligned}
 \|\mathbb{E}[\delta_2^*]\| &= \|\mathbb{E}[\tilde{\nabla} f_i(\theta - \alpha \tilde{\nabla} f_i(\theta, \mathcal{D}_i), \mathcal{D}_i') - \nabla f_i(\theta - \alpha \tilde{\nabla} f_i(\theta, \mathcal{D}_i)) + \nabla f_i(\theta - \alpha \tilde{\nabla} f_i(\theta, \mathcal{D}_i)) - \nabla f_i(\theta - \alpha \nabla f_i(\theta))]\| \\
 &= \|\mathbb{E}[\nabla f_i(\theta - \alpha \tilde{\nabla} f_i(\theta, \mathcal{D}_i)) - \nabla f_i(\theta - \alpha \nabla f_i(\theta))]\| \quad (\text{from the tower rule and independence between } \mathcal{D} \text{ and } \mathcal{D}') \\
 &\leq \mathbb{E}[\|\nabla f_i(\theta - \alpha \tilde{\nabla} f_i(\theta, \mathcal{D}_i)) - \nabla f_i(\theta - \alpha \nabla f_i(\theta))\|] \\
 &\leq \alpha L \mathbb{E}[\|\tilde{\nabla} f_i(\theta, \mathcal{D}_i) - \nabla f_i(\theta)\|] \quad (\text{from the smoothness of } f_i) \\
 &\leq \frac{\alpha \sigma_G L}{\sqrt{D_i}}. \quad (\text{from Assumption 3})
 \end{aligned}$$

Regarding the second moment, we have

$$\begin{aligned}
 \mathbb{E}[\|\delta_2^*\|^2] &\leq 2\mathbb{E}[\|\tilde{\nabla} f_i(\theta - \alpha \tilde{\nabla} f_i(\theta, \mathcal{D}_i), \mathcal{D}_i') - \nabla f_i(\theta - \alpha \tilde{\nabla} f_i(\theta, \mathcal{D}_i))\|^2] + 2\mathbb{E}[\|\nabla f_i(\theta - \alpha \tilde{\nabla} f_i(\theta, \mathcal{D}_i)) - \nabla f_i(\theta - \alpha \nabla f_i(\theta))\|^2] \\
 &\leq \frac{2\sigma_G^2}{D_i'} + 2(\alpha L)^2 \mathbb{E}[\|\tilde{\nabla} f_i(\theta, \mathcal{D}_i) - \nabla f_i(\theta)\|] \quad (\text{from the tower rule, smoothness of } f_i \text{ along with Assumption 3})
 \end{aligned}$$

$$\leq 2\sigma_G^2 \left(\frac{1}{D'_i} + \frac{(\alpha L)^2}{D_i} \right). \quad (64)$$

Based on (59), we have

$$\begin{aligned} \|\mathbb{E} [\tilde{\nabla} F_i \theta - \nabla F_i(\theta)]\| &= \left\| \left(I - \alpha \nabla^2 f_i(\theta) \right) \mathbb{E}[\delta_2^*] + \mathbb{E}[\delta_1^*] \nabla f_i(\theta - \alpha \nabla f_i(\theta)) + \mathbb{E}[\delta_1^* \delta_2^*] \right\| \\ &\leq \|I - \alpha \nabla^2 f_i(\theta)\| \|\mathbb{E}[\delta_2^*]\| \quad (\text{from (62) and submultiplicative property of matrix norm}) \\ &\leq \frac{\alpha \sigma_G L (1 + \alpha L)}{\sqrt{D_i}}, \end{aligned} \quad (65)$$

which gives us the first result in Lemma 2.

By the submultiplicative property of matrix norm, we can write

$$\|\tilde{\nabla} F_i \theta - \nabla F_i(\theta)\| \leq \|I - \alpha \nabla^2 f_i(\theta)\| \|\delta_2^*\| + \|\nabla f_i(\theta - \alpha \nabla f_i(\theta))\| \|\delta_1^*\| + \|\delta_1^*\| \|\delta_2^*\|. \quad (66)$$

Thus, we have

$$\|\tilde{\nabla} F_i \theta - \nabla F_i(\theta)\|^2 \leq 3 \|I - \alpha \nabla^2 f_i(\theta)\|^2 \|\delta_2^*\|^2 + 3 \|\nabla f_i(\theta - \alpha \nabla f_i(\theta))\|^2 \|\delta_1^*\|^2 + 3 \|\delta_1^*\|^2 \|\delta_2^*\|^2. \quad (67)$$

Taking expectation from both sides, we obtain

$$\begin{aligned} \mathbb{E} [\|\tilde{\nabla} F_i \theta - \nabla F_i(\theta)\|^2] &\leq 3 (1 + \alpha L)^2 \mathbb{E} [\|\delta_2^*\|^2] + 3 \zeta^2 \mathbb{E} [\|\delta_1^*\|^2] + 3 \mathbb{E} [\|\delta_1^*\|^2] \mathbb{E} [\|\delta_2^*\|^2] \\ &\quad (\text{using the fact that } \|I - \alpha \nabla^2 f_i(\theta)\| \leq 1 + \alpha L) \\ &\leq \frac{6(\alpha \sigma_G \sigma_H)^2}{D''_i} \left(\frac{1}{D'_i} + \frac{(\alpha L)^2}{D_i} \right) + 6\sigma_G^2 (1 + \alpha L)^2 \left(\frac{1}{D'_i} + \frac{(\alpha L)^2}{D_i} \right) + \frac{3(\alpha \zeta \sigma_H)^2}{D''_i}, \end{aligned} \quad (68)$$

which completes the proof.

APPENDIX C PROOF OF LEMMA 3

Recall the definition of $F_i(\theta)$. We have

$$\begin{aligned} \|\nabla F_i(\theta) - F_j(\theta)\| &= \left\| \left(I - \alpha \nabla^2 f_i(\theta) \right) \nabla f_i(\theta - \alpha \nabla f_i(\theta)) - \left(I - \alpha \nabla^2 f_j(\theta) \right) \nabla f_j(\theta - \alpha \nabla f_j(\theta)) \right\| \\ &\leq \left\| \left(I - \alpha \nabla^2 f_i(\theta) \right) \nabla f_i(\theta - \alpha \nabla f_i(\theta)) - \left(I - \alpha \nabla^2 f_j(\theta) \right) \nabla f_i(\theta - \alpha \nabla f_i(\theta)) \right\| \\ &\quad + \left\| \left(I - \alpha \nabla^2 f_j(\theta) \right) \nabla f_i(\theta - \alpha \nabla f_i(\theta)) - \left(I - \alpha \nabla^2 f_j(\theta) \right) \nabla f_j(\theta - \alpha \nabla f_j(\theta)) \right\| \\ &\leq \underbrace{\alpha \left\| \left(\nabla^2 f_i(\theta) - \nabla^2 f_j(\theta) \right) \nabla f_i(\theta - \alpha \nabla f_i(\theta)) \right\|}_A \\ &\quad + \underbrace{\left\| \left(I - \alpha \nabla^2 f_j(\theta) \right) \left(\nabla f_i(\theta - \alpha \nabla f_i(\theta)) - \nabla f_j(\theta - \alpha \nabla f_j(\theta)) \right) \right\|}_B. \end{aligned} \quad (69)$$

Regrading A , due to the submultiplicative property of matrix norm, the following holds

$$\begin{aligned} A &\leq \|\nabla^2 f_i(\theta) - \nabla^2 f_j(\theta)\| \|\nabla f_i(\theta - \alpha \nabla f_i(\theta))\| \\ &\leq \zeta \gamma_H, \end{aligned} \quad (70)$$

where the last inequality follows from Assumption 4.

Regrading B , similarly, we obtain

$$\begin{aligned} B &\leq \|I - \alpha \nabla^2 f_j(\theta)\| \|\nabla f_i(\theta - \alpha \nabla f_i(\theta)) - \nabla f_j(\theta - \alpha \nabla f_j(\theta))\| \\ &\stackrel{(a)}{\leq} (1 + \alpha L) \|\nabla f_i(\theta - \alpha \nabla f_i(\theta)) - \nabla f_j(\theta - \alpha \nabla f_j(\theta))\| \\ &\leq (1 + \alpha L) \left(\|\nabla f_i(\theta - \alpha \nabla f_i(\theta)) - \nabla f_i(\theta - \alpha \nabla f_j(\theta))\| \right. \\ &\quad \left. + \|\nabla f_i(\theta - \alpha \nabla f_j(\theta)) - \nabla f_j(\theta - \alpha \nabla f_j(\theta))\| \right) \\ &\stackrel{(b)}{\leq} (1 + \alpha L) (\alpha L \|\nabla f_i(\theta) - f_j(\theta)\| + \gamma_G) \\ &\leq (1 + \alpha L)^2 \gamma_G, \end{aligned} \quad (71)$$

where (a) is derived via triangle inequality, and (b) follows from Assumptions 1 and 4.

Substituting (70) and (71) in (69), we can write

$$\|\nabla F_i(\theta) - F_j(\theta)\| \leq (1 + \alpha L)^2 \gamma_G + \alpha \zeta \gamma_H, \quad (72)$$

thereby completing the proof.

APPENDIX D PROOF OF LEMMA 4

Since j is the straggler among users, (SP1) can be equivalently transformed to the following one

$$\begin{aligned} \min_{\nu} \quad & \eta_1 \sum_{i \in \mathcal{N}} \frac{\iota_i}{2} c_i D_i \nu_i^2 + \eta_2 \frac{c_j D_j}{\nu_j} \\ \text{s.t.} \quad & 0 \leq \nu_i \leq \nu_i^{\max}, \quad \forall i \in \mathcal{N}, \\ & \frac{c_i D_i \nu_j}{c_j D_j} \leq \nu_i, \quad \forall i \in \mathcal{N}/j. \end{aligned} \quad (73)$$

Fixing ν_j , for each $i \in \mathcal{N}/j$ ⁴, we can easily show that the optimal CPU frequency ν_i^* of the problem (73) (slightly abusing notations here) can be obtained via solving the following decomposed convex optimization problem

$$\begin{aligned} \min_{\nu_i} \quad & \frac{\iota_i}{2} \eta_1 c_i D_i \nu_i^2 \\ \text{s.t.} \quad & 0 \leq \nu_i \leq \nu_i^{\max}, \\ & \frac{c_i D_i \nu_j}{c_j D_j} \leq \nu_i. \end{aligned} \quad (74)$$

If $\nu_j \leq \frac{c_j D_j \nu_i^{\max}}{c_i D_i}$ holds, then the optimal solution of the problem (74) can be expressed as

$$\nu_i^* = \frac{c_i D_i \nu_j}{c_j D_j}. \quad (75)$$

Otherwise, the problem is infeasible because the constraints are mutually contradictory. Substituting $\nu_i = \nu_i^*$ in the problem (73), we have the following problem with respect to ν_j

$$\begin{aligned} \min_{\nu_j} \quad & g(\nu_j) = \eta_1 \underbrace{\left(\sum_{i \in \mathcal{N}/j} \frac{\iota_i (c_i D_i)^3}{2(c_j D_j)^2} + \frac{\iota_j c_j D_j}{2} \right) \nu_j^2}_{a_1} + \underbrace{\eta_2 c_j D_j}_{a_2} \frac{1}{\nu_j} \\ \text{s.t.} \quad & 0 \leq \nu_j \leq \frac{c_j D_j \nu_i^{\max}}{c_i D_i}, \quad \forall i \in \mathcal{N}. \end{aligned} \quad (76)$$

We simplify the expression of $g(\nu_j)$ as $g(\nu_j) = a_1 \nu_j^2 + a_2 / \nu_j$ where the positive constants a_1 and a_2 are defined in (76). Then, the derivative of $g(\nu_j)$ can be written as follows

$$g'(\nu_j) = 2a_1 \nu_j - \frac{a_2}{\nu_j^2}. \quad (77)$$

Based on (77), it is easy to see that the minimum value of $g(\nu_j)$ is obtained at its stationary point $\bar{\nu}_j := g'^{-1}(0) = \sqrt[3]{\frac{a_2}{2a_1}}$. Thus, the optimal solution of the problem (76) is

$$\nu_j^* = \min \left\{ \sqrt[3]{\frac{a_2}{2a_1}}, \min_{i \in \mathcal{N}} \frac{c_j D_j \nu_i^{\max}}{c_i D_i} \right\}. \quad (78)$$

Combining (75) and (78), we complete the proof.

⁴We implicitly assume that \mathcal{N}/j is not empty.

APPENDIX E
PROOF OF LEMMA 5

Given z^* and δ^* , p_i^* can be obtained via solving the following problem

$$\begin{aligned} \min_{p_i} \quad & \sum_{m \in \mathcal{M}} \frac{z_{i,m}^* p_i}{\log_2 \left(1 + \frac{h_i p_i}{I_m + BN_0} \right)} \\ \text{s.t.} \quad & 0 \leq p_i \leq p_i^{\max}, \\ & \sum_{m \in \mathcal{M}} \frac{z_{i,m}^* S}{B \log_2 \left(1 + \frac{h_i p_i}{I_m + BN_0} \right)} \leq \delta^*, \end{aligned} \quad (79)$$

where we eliminate u_i , η_1 , S , and B in the objective. Clearly, if $\sum_{m \in \mathcal{M}} z_{i,m}^* = 0$, then $p_i^* = 0$. Besides, it can be easily shown that if the constraints in (79) are mutually contradictory, *i.e.*

$$p_i^{\max} < \frac{(I_{m_i^*} + BN_0)(2^{\frac{S}{B\delta^*}} - 1)}{h_i}, \quad (80)$$

then $z_{i,m}^*$ must be 0, which gives (41).

When there exists m_i^* such that $z_{i,m_i^*}^* = 1$, by denoting $\tilde{p}_i := \frac{h_i p_i}{I_{m_i^*} + BN_0}$ and rearranging the terms, we can transform the problem (79) to the following one

$$\begin{aligned} \min_{\tilde{p}_i} \quad & g_3(\tilde{p}_i) = \frac{\tilde{p}_i}{\log_2(1 + \tilde{p}_i)} \\ \text{s.t.} \quad & 0 \leq \tilde{p}_i \leq \frac{h_i p_i^{\max}}{I_{m_i^*} + BN_0}, \\ & 2^{\frac{S}{B\delta^*}} - 1 \leq \tilde{p}_i. \end{aligned} \quad (81)$$

It is easy to see that

$$g_3'(\tilde{p}_i) = \frac{\log_2(1 + \tilde{p}_i) - \tilde{p}_i / ((1 + \tilde{p}_i) \ln 2)}{(\log_2(1 + \tilde{p}_i))^2}. \quad (82)$$

Denoting the numerator of (82) as $f_3(\tilde{p}_i)$, we have $f_3(0) = 0$ and

$$f_3'(\tilde{p}_i) = \frac{1}{\ln 2} \left(\frac{1}{(1 + \tilde{p}_i)} - \frac{1}{(1 + \tilde{p}_i)^2} \right) > 0, \quad \text{when } \tilde{p}_i > 0, \quad (83)$$

which implies that $g_3(\tilde{p}_i)$ is monotonically increasing with $\tilde{p}_i > 0$. Thus, recalling the definition of \tilde{p}_i , due to (41), we obtain

$$p_i^* = \frac{(I_{m_i^*} + BN_0)(2^{\frac{S}{B\delta^*}} - 1)}{h_i}, \quad (84)$$

which completes the proof of (42).

APPENDIX F
PROOF OF LEMMA 6

If j denotes the straggler among all users and $\mathcal{N}^* \neq \emptyset$, then we can rewrite (45) for each $i \in \mathcal{N}^*$ as

$$\begin{aligned} & \sum_{m \in \mathcal{M}} z_{i,m}^* \frac{S}{B \log_2 \left(1 + \frac{h_i p_i^*}{I_m + BN_0} \right)} \leq \sum_{m \in \mathcal{M}} z_{j,m}^* \frac{S}{B \log_2 \left(1 + \frac{h_j p_j^*}{I_m + BN_0} \right)} \\ \Leftrightarrow \quad & \log_2 \left(1 + \frac{h_j p_j^*}{I_{m_j^*} + BN_0} \right) \leq \log_2 \left(1 + \frac{h_i p_i^*}{I_{m_i^*} + BN_0} \right) \\ \Leftrightarrow \quad & \frac{(I_{m_i^*} + BN_0)h_j}{(I_{m_j^*} + BN_0)h_i} p_j^* \leq p_i^*. \end{aligned} \quad (85)$$

Based on (85), by eliminating constants B and S , we transform (SP2) under fixed z^* to the following equivalent problem

$$\begin{aligned} \min_{\{p_i\}_{i \in \mathcal{N}^*}} \quad & \sum_{i \in \mathcal{N}^*} \eta_1 \frac{p_i}{\log_2 \left(1 + \frac{h_i p_i}{I_{m_i^*} + BN_0} \right)} + \eta_2 \frac{1}{\log_2 \left(1 + \frac{h_j p_j}{I_{m_j^*} + BN_0} \right)} \\ \text{s.t.} \quad & 0 \leq p_i \leq p_i^{\max}, \quad \forall i \in \mathcal{N}^*, \\ & \frac{(I_{m_i^*} + BN_0)h_j}{(I_{m_j^*} + BN_0)h_i} p_j \leq p_i, \quad \forall i \in \mathcal{N}^*/j. \end{aligned} \quad (86)$$

Due to (85), for each $i \in \mathcal{N}^*/j$, we can obtain the optimal solution p_i^* of (86) (abusing notations) via solving the decomposed problem as follows

$$\begin{aligned} \min_{\tilde{p}_i} \quad & g_3(\tilde{p}_i) = \frac{\tilde{p}_i}{\log_2(1 + \tilde{p}_i)} \\ \text{s.t.} \quad & 0 \leq \tilde{p}_i \leq \frac{h_i p_i^{\max}}{I_{m_i^*} + BN_0}, \\ & \frac{h_j}{I_{m_j^*} + BN_0} p_j \leq \tilde{p}_i, \end{aligned} \quad (87)$$

where $\tilde{p}_i := \frac{h_i p_i}{I_{m_i^*} + BN_0}$. Note that in (87) we consider the nontrivial case where \mathcal{N}/j is not empty. It is easy to see that

$$g_3'(\tilde{p}_i) = \frac{\log_2(1 + \tilde{p}_i) - \tilde{p}_i / ((1 + \tilde{p}_i) \ln 2)}{(\log_2(1 + \tilde{p}_i))^2}. \quad (88)$$

Denote the numerator of (88) as $f_3(\tilde{p}_i)$. Then, we have $f_3(0) = 0$ and

$$f_3'(\tilde{p}_i) = \frac{1}{\ln 2} \left(\frac{1}{(1 + \tilde{p}_i)} - \frac{1}{(1 + \tilde{p}_i)^2} \right) > 0, \quad \text{when } \tilde{p}_i > 0, \quad (89)$$

which implies that $g_3(\tilde{p}_i)$ is monotonically increasing with $\tilde{p}_i > 0$. Thus, if $p_j \leq \frac{h_i p_i^{\max} (I_{m_j^*} + BN_0)}{h_j (I_{m_i^*} + BN_0)}$, recalling the definition of \tilde{p}_i , we have

$$p_i^* = \frac{h_j (I_{m_i^*} + BN_0)}{h_i (I_{m_j^*} + BN_0)} p_j, \quad \forall i \in \mathcal{N}^*/j. \quad (90)$$

Otherwise, the problem (87) is infeasible.

Similar to (87), We denote $\tilde{p}_j := \frac{h_j p_j}{I_{m_j^*} + BN_0}$ and institute $p_i = p_i^*$ in (86) (noting that $p_i = \frac{(I_{m_i^*} + BN_0) \tilde{p}_j}{h_i}$), whereby we have the following problem regarding \tilde{p}_j

$$\begin{aligned} \min_{\tilde{p}_j} \quad & g_4(\tilde{p}_j) = \eta_1 \underbrace{\sum_{i \in \mathcal{N}^*} \frac{I_{m_i^*} + BN_0}{h_i} \cdot \frac{\tilde{p}_j}{\log_2(1 + \tilde{p}_j)}}_{b_1} + \frac{\eta_2}{\log_2(1 + \tilde{p}_j)} \\ \text{s.t.} \quad & 0 \leq \tilde{p}_j \leq \frac{h_i p_i^{\max}}{I_{m_i^*} + BN_0}, \quad \forall i \in \mathcal{N}^*. \end{aligned} \quad (91)$$

Denoting positive constant b_1 as in (91), we can write $g_4(\tilde{p}_j) = \frac{b_1 \tilde{p}_j}{\log_2(1 + \tilde{p}_j)} + \frac{\eta_2}{\log_2(1 + \tilde{p}_j)}$ and obtain

$$\begin{aligned} g_4'(\tilde{p}_j) &= b_1 g_3'(\tilde{p}_j) - \frac{\eta_2}{(1 + \tilde{p}_j) (\log_2(1 + \tilde{p}_j))^2 \ln 2} \\ &= b_1 \frac{\log_2(1 + \tilde{p}_j) - \tilde{p}_j / ((1 + \tilde{p}_j) \ln 2)}{(\log_2(1 + \tilde{p}_j))^2} - \frac{\eta_2}{(1 + \tilde{p}_j) (\log_2(1 + \tilde{p}_j))^2 \ln 2} \\ &= \frac{b_1 ((1 + \tilde{p}_j) \log_2(1 + \tilde{p}_j) \ln 2 - \tilde{p}_j) - \eta_2}{(1 + \tilde{p}_j) (\log_2(1 + \tilde{p}_j))^2 \ln 2}. \end{aligned} \quad (92)$$

Next, we show that $g_4(\tilde{p}_j)$ has unique minimum point. We first denote the numerator of (92) as $f_4(\tilde{p}_j)$. Then, we have $f_4(0) = -\eta_2 \leq 0$ and

$$f_4'(\tilde{p}_j) = b_1 \log_2(1 + \tilde{p}_j) \ln 2 \geq 0, \quad \text{when } \tilde{p}_j \geq 0, \quad (93)$$

which implies $f_4(\tilde{p}_j)$ is monotonically increasing. Besides, it can be easily shown that $f_4(b_2) \geq 0$, where $b_2 = 2^{(1+\sqrt{\max\{\frac{\eta_2}{b_1}, 1\}-1})/\ln 2}$. Thus, there must exist a unique point $\tilde{p}_j^0 \in (0, b_2]$ such that $g_4'(\tilde{p}_j^0) = f_4(\tilde{p}_j^0) = 0$ holds, and it is also the minimum value of $g_4(\tilde{p}_j)$.

Based on that, the optimal solution of the problem (91) can be expressed as

$$\tilde{p}_j^* = \min \left\{ \tilde{p}_j^0, \min_{i \in \mathcal{N}^*} \frac{h_i p_i^{\max}}{I_{m_i^*} + BN_0} \right\}. \quad (94)$$

Therefore, we complete the proof.

APPENDIX G PROOF OF THEOREM 3

From Lemma 5, it can be easily seen that (43) holds if $\mu_{i,m} \leq p_i^{\max}$. On the other hand, when $\mu_{i,m} > p_i^{\max}$, if device i is selected, the transmission delay will be larger than δ^* (see the proof of Lemma 5), which is contradictory to the given condition. Thus, when $\mu_{i,m} > p_i^{\max}$, we set $e_{i,m} = u_i + 1$, enabling device i not to be selected.

APPENDIX H PROOF OF THEOREM 1

Due to Lemma 1 (smoothness of F_i), it can be shown that for any $\theta_1, \theta_2 \in \mathbb{R}^d$, the following fact holds

$$F(\theta_2) \leq F(\theta_1) + \nabla F(\theta_1)^\top (\theta_2 - \theta_1) + \frac{L_F}{2} \|\theta_2 - \theta_1\|^2. \quad (95)$$

Combining (95) with (2), we have

$$\begin{aligned} F(\theta^{k+1}) &\leq F(\theta^k) + \nabla F(\theta^k)^\top (\theta^{k+1} - \theta^k) + \frac{L_F}{2} \|\theta^{k+1} - \theta^k\|^2 \\ &= F(\theta^k) - \beta \nabla F(\theta^k)^\top \left(\frac{1}{n_k} \sum_{i \in \mathcal{N}_k} \tilde{\nabla} F_i(\theta^k) \right) + \frac{L_F \beta^2}{2} \left\| \frac{1}{n_k} \sum_{i \in \mathcal{N}_k} \tilde{\nabla} F_i(\theta^k) \right\|^2. \end{aligned} \quad (96)$$

We denote G^k as

$$G^k := \beta \nabla F(\theta^k)^\top \left(\frac{1}{n_k} \sum_{i \in \mathcal{N}_k} \tilde{\nabla} F_i(\theta^k) \right) - \frac{L_F \beta^2}{2} \left\| \frac{1}{n_k} \sum_{i \in \mathcal{N}_k} \tilde{\nabla} F_i(\theta^k) \right\|^2. \quad (97)$$

It is easy to see that $\mathbb{E}[F(\theta^k) - F(\theta^{k+1})] \geq \mathbb{E}[G^k]$. Next, we bound $\mathbb{E}[G^k]$ from below.

First, for any $i \in \mathcal{N}$ we rewrite $\nabla F(\theta^k)$ as follows

$$\nabla F(\theta^k) = \underbrace{\frac{1}{n} \sum_{j \in \mathcal{N}} \nabla F_j(\theta^k) - \nabla F_i(\theta^k)}_{A_i} + \underbrace{\nabla F_i(\theta^k) - \tilde{\nabla} F_i(\theta^k) + \tilde{\nabla} F_i(\theta^k)}_{B_i}, \quad (98)$$

and we can bound $\mathbb{E}[\|A_i\|^2]$ by

$$\begin{aligned} \mathbb{E}[\|A_i\|^2] &= \mathbb{E} \left[\left\| \nabla F_i(\theta^k) - \frac{1}{n} \sum_{j \in \mathcal{N}} \nabla F_j(\theta^k) \right\|^2 \right] \\ &= \mathbb{E} \left[\left\| \frac{1}{n} \sum_{j \in \mathcal{N}} (\nabla F_j(\theta^k) - \nabla F_i(\theta^k)) \right\|^2 \right] \\ &\stackrel{(a)}{\leq} \frac{1}{n} \sum_{j \in \mathcal{N}} \mathbb{E} \left[\left\| \nabla F_j(\theta^k) - \nabla F_i(\theta^k) \right\|^2 \right] \\ &\stackrel{(b)}{\leq} (1 + \alpha L)^2 \gamma_G + \alpha \zeta \gamma_H, \end{aligned} \quad (99)$$

where (b) is derived from Lemma 3. Inequality (a) follows from the fact that for any $a_i \in \mathbb{R}^d$ and $b_i \in \mathbb{R}$

$$\begin{aligned} \left\| \sum_{i \in \mathcal{N}_k} b_i a_i \right\|^2 &= \sum_{j=1}^d \left(\sum_{i \in \mathcal{N}_k} b_i a_i^{(j)} \right)^2 \\ &\leq \sum_{j=1}^d \left(\sum_{i \in \mathcal{N}_k} (a_i^{(j)})^2 \right) \left(\sum_{i \in \mathcal{N}_k} b_i^2 \right) \end{aligned}$$

$$\begin{aligned}
&= \left(\sum_{j=1}^d \sum_{i \in \mathcal{N}_k} \left(a_i^{(j)} \right)^2 \right) \left(\sum_{i \in \mathcal{N}_k} b_i^2 \right) \\
&= \left(\sum_{i \in \mathcal{N}_k} \|a_i\|^2 \right) \left(\sum_{i \in \mathcal{N}_k} b_i^2 \right),
\end{aligned} \tag{100}$$

where $a_i^{(j)}$ denotes the j -th coordinate of a_i , and the first inequality is derived by Cauchy-Schwarz inequality.

Regarding $\mathbb{E}[\|B_i\|^2]$, due to Lemma 2, it is easy to see that

$$\mathbb{E}[\|B_i\|^2] \leq \sigma_{F_i}^2. \tag{101}$$

Based on that, substituting (98) in $\mathbb{E}[G^k]$, we can obtain

$$\begin{aligned}
\mathbb{E}[G^k] &= \mathbb{E} \left[\beta \nabla F(\theta^k)^\top \left(\frac{1}{n_k} \sum_{i \in \mathcal{N}_k} \tilde{\nabla} F_i(\theta^k) \right) - \frac{L_F \beta^2}{2} \left\| \frac{1}{n_k} \sum_{i \in \mathcal{N}_k} \tilde{\nabla} F_i(\theta^k) \right\|^2 \right] \\
&= \mathbb{E} \left[\frac{\beta}{n_k} \sum_{i \in \mathcal{N}_k} \left(A_i + B_i + \tilde{\nabla} F_i(\theta^k) \right)^\top \tilde{\nabla} F_i(\theta^k) - \frac{L_F \beta^2}{2} \left\| \frac{1}{n_k} \sum_{i \in \mathcal{N}_k} \tilde{\nabla} F_i(\theta^k) \right\|^2 \right] \\
&= \mathbb{E} \left[\frac{\beta}{n_k} \sum_{i \in \mathcal{N}_k} \left(A_i^\top \tilde{\nabla} F_i(\theta^k) + B_i^\top \tilde{\nabla} F_i(\theta^k) + \|\tilde{\nabla} F_i(\theta^k)\|^2 \right) \right] - \frac{L_F \beta^2}{2} \mathbb{E} \left[\left\| \frac{1}{n_k} \sum_{i \in \mathcal{N}_k} \tilde{\nabla} F_i(\theta^k) \right\|^2 \right].
\end{aligned} \tag{102}$$

Note that for any random variables $a, b \in \mathbb{R}^d$, the following inequality holds for $c \neq 0$

$$\mathbb{E}[a^\top b] \geq -\mathbb{E} \left[2 \left\| (ca)^\top \frac{b}{2c} \right\| \right] \geq - \left(c^2 \mathbb{E}[\|a\|^2] + \frac{\mathbb{E}[\|b\|^2]}{4c^2} \right). \tag{103}$$

If we define $g(x) := x \mathbb{E}[\|a\|^2] + \mathbb{E}[\|b\|^2]/(4x)$, then it can be easily shown that

$$x^* = \arg \min_x g(x) = \sqrt{\frac{\mathbb{E}[\|b\|^2]}{4\mathbb{E}[\|a\|^2]}}, \tag{104}$$

which implies that if we set $c^2 = x^*$, then the lower bound in (103) becomes tight. Thus, substituting this in (103) and rearranging the terms, we have

$$\mathbb{E}[a^\top b] \geq -\sqrt{\mathbb{E}[\|a\|^2] \mathbb{E}[\|b\|^2]}. \tag{105}$$

Based on (105) along with (100), due to the tower rule, we can bound $\mathbb{E}[G^k]$ as follows

$$\begin{aligned}
\mathbb{E}[G^k] &= \mathbb{E} \left[\frac{\beta}{n_k} \sum_{i \in \mathcal{N}_k} \left(A_i^\top \tilde{\nabla} F_i(\theta^k) + B_i^\top \tilde{\nabla} F_i(\theta^k) + \|\tilde{\nabla} F_i(\theta^k)\|^2 \right) \right] - \frac{L_F \beta^2}{2} \mathbb{E} \left[\left\| \frac{1}{n_k} \sum_{i \in \mathcal{N}_k} \tilde{\nabla} F_i(\theta^k) \right\|^2 \right] \quad (\text{from (102)}) \\
&= \mathbb{E} \left[\frac{\beta}{n_k} \sum_{i \in \mathcal{N}_k} \left(\mathbb{E} \left[A_i^\top \tilde{\nabla} F_i(\theta^k) \middle| \mathcal{N}_k \right] + \mathbb{E} \left[B_i^\top \tilde{\nabla} F_i(\theta^k) \middle| \mathcal{N}_k \right] + \|\tilde{\nabla} F_i(\theta^k)\|^2 \right) \right] \\
&\quad - \frac{L_F \beta^2}{2} \mathbb{E} \left[\left\| \frac{1}{n_k} \sum_{i \in \mathcal{N}_k} \tilde{\nabla} F_i(\theta^k) \right\|^2 \right] \quad (\text{using the tower rule}) \\
&\geq \mathbb{E} \left[\frac{\beta}{n_k} \sum_{i \in \mathcal{N}_k} \left(-\sqrt{\mathbb{E}[\|A_i\|^2 \mid \mathcal{N}_k]} \sqrt{\mathbb{E}[\|\tilde{\nabla} F_i(\theta^k)\|^2 \mid \mathcal{N}_k]} - \sqrt{\mathbb{E}[\|B_i\|^2 \mid \mathcal{N}_k]} \sqrt{\mathbb{E}[\|\tilde{\nabla} F_i(\theta^k)\|^2 \mid \mathcal{N}_k]} \right) \right] \\
&\quad + \beta \left(1 - \frac{L_F \beta}{2} \right) \mathbb{E} \left[\frac{1}{n_k} \sum_{i \in \mathcal{N}_k} \|\tilde{\nabla} F_i(\theta^k)\|^2 \right] \quad (\text{using (105) and (100), and rearranging terms}) \\
&\geq \mathbb{E} \left[\frac{\beta}{n_k} \sum_{i \in \mathcal{N}_k} - \left(\sqrt{(1 + \alpha L)^2 \gamma_G + \alpha \zeta \gamma_H} + \sigma_{F_i} \right) \sqrt{\mathbb{E}[\|\tilde{\nabla} F_i(\theta^k)\|^2 \mid \mathcal{N}_k]} \right] \quad (\text{from (99) and (101)}) \\
&\quad + \beta \left(1 - \frac{L_F \beta}{2} \right) \mathbb{E} \left[\frac{1}{n_k} \sum_{i \in \mathcal{N}_k} \|\tilde{\nabla} F_i(\theta^k)\|^2 \right]
\end{aligned}$$

$$= \beta \mathbb{E} \left[\frac{1}{n_k} \sum_{i \in \mathcal{N}_k} \left(1 - \frac{L_F \beta}{2} \right) \|\tilde{\nabla} F_i(\theta^k)\|^2 - \left(\sqrt{(1 + \alpha L)^2 \gamma_G + \alpha \zeta \gamma_H} + \sigma_{F_i} \right) \sqrt{\mathbb{E} \left[\|\tilde{\nabla} F_i(\theta^k)\|^2 \middle| \mathcal{N}_k \right]} \right], \quad (106)$$

thereby completing the proof.

APPENDIX I PROOF OF THEOREM 5

First, it is easy to see that $g_2(\mathbf{z}, \mathbf{p})$ is upper bounded by $\sum_{i \in \mathcal{N}} u_i$. Besides, due to (43), we have

$$\mathbf{z}^{t+1} = \arg \max_{\mathbf{z}} \left\{ \sum_{i \in \mathcal{N}} \sum_{m \in \mathcal{M}} z_{i,m} \left(u_i - \frac{\eta_1 \delta^t (I_m + BN_0) (2^{\frac{S}{B\delta^t}} - 1)}{h_i} \right), \text{ s.t. (26) - (35)} \right\}. \quad (107)$$

Based on (48), we define the optimal transmission power $\hat{\mathbf{p}}^{t+1}$ corresponding to \mathbf{z}^{t+1} as follows

$$\hat{p}_i^{t+1} = \begin{cases} \frac{(I_{m_i^*} + BN_0) (2^{\frac{S}{B\delta^t}} - 1)}{h_i} & , \text{ if } \sum_{m \in \mathcal{M}} z_{i,m}^{t+1} = 1, \\ 0 & , \text{ otherwise,} \end{cases} \quad (108)$$

where we slightly abuse the notation and denote the RB block allocated to i as m_i^* , i.e., $z_{i,m_i^*}^{t+1} = 1$. Thus, we have $g(\mathbf{z}^t, \mathbf{p}^t) \leq g(\mathbf{z}^{t+1}, \hat{\mathbf{p}}^{t+1})$. Due to (49), it can be easily shown that $g(\mathbf{z}^{t+1}, \hat{\mathbf{p}}^{t+1}) \leq g(\mathbf{z}^{t+1}, \mathbf{p}^{t+1})$. Using these two inequalities, we obtain

$$g(\mathbf{z}^t, \mathbf{p}^t) \leq g(\mathbf{z}^{t+1}, \mathbf{p}^{t+1}), \quad (109)$$

thereby completing the proof.

APPENDIX J PROOF OF COROLLARIES 1 AND 2

The result of Corollary 1 can be directly derived by plugging (15) into the RHS of (17) and summing up for $t = 0, \dots, \tau - 1$.

The result of Corollary 2 can be also easily shown via combining [11, Lemma H.1] and [11, Lemma H.2] with the proof of Lemma 1.